Student thesis series INES nr 670

Fungal necromass decomposition dynamics is driven by fungal physiological state at death

Danny Lopes Ramos

2024
Department of
Physical Geography and Ecosystem Science
Lund University
Sölvegatan 12
S-223 62 Lund
Sweden

Danny Lopes Ramos (2024).
Fungal necromass decomposition dynamics is driven by fungal physiological state at death.
Master degree thesis, 30 credits in *Physical Geography & Ecosystem Sciences*
Department of Physical Geography and Ecosystem Science, Lund University

Level: Master of Science (MSc)

Course duration: *January* 2024 until *June* 2024

Fungal necromass decomposition dynamics is driven by fungal physiological state at death

---

Danny Lopes Ramos

Master thesis, 30 credits, in *Physical Geography & Ecosystem Sciences*

Supervisor : François Maillard
Lund University

Supervisor: Anders Tunlid
Lund University

Exam committee:
Annemarie Eckes-Shepard, Lund University
Håkan Wallander, Lund University

LUNDS UNIVERSITET

Danny Lopes Ramos
Physical Geography and Ecosystem Science
Lund University
August 19, 2024

Master's Thesis

Fungal necromass decomposition dynamics is driven by fungal physiological state at death

Abstract

Soil organic matter is a critical component of terrestrial ecosystems, with a significant role in mitigating climate change. Understanding the formation and decomposition of soil organic carbon is essential for accurately predicting the carbon cycle and developing sustainable agricultural and silvicultural practices. In this context, the decomposition dynamics of fungal dead mycelial residues, or necromass, have been the subject of growing scientific interest. Fungal necromass can make up more than half of the stable SOC, but its decomposition dynamics are not well understood, particularly regarding the physiological state of the fungi at death. In this project, I aimed to test how the fungal physiological state at death affects the subsequent decomposition of the necromass. I conducted an experiment using *Neurospora crassa*, a fungus commonly found in soil, by burying mesh bags filled with fungal necromass and sequentially collecting them over four months. In our fungal necromass study, I confronted two distinct decomposition models, based on recent research, and computed their decay parameters, while also examining alternatives from plant litter studies. Additionally, I used Diffuse Reflectance Infrared Fourier Transform Spectroscopy analysis to quantify the biochemical composition of the fungal necromass initially and during decomposition, suggesting that fungal compounds were driving the decomposition process. Our results showed that fungal biomass became more enriched in cell-wall compounds relative to non-structural compounds as the physiological age at death of *Neurospora crassa* progressed, but the oldest necromass age did not follow this trend. This enrichment in structural compounds led to a decrease in fungal necromass decay rates and a larger fraction of fungal necromass resistant to microbial decomposition. These findings have important implications for understanding the role of fungi in SOC formation and developing sustainable land-use practices.

Contents

List of Figures

List of Tables

List of Abbreviation

AIC_c	Akaike Information Criterion
ANOVA	Analysis of Variance
C	Carbon
CO_2	Carbon Dioxide
DRIFTS	Diffuse Reflectance Infrared Fourier Transform Spectroscopy
FTIR	Fourier Transform Infrared Spectroscopy
GC-MS	Gas Chromatography-Mass Spectrometry
H	Hydrogen
MAOM	Mineral Associated Organic Matter
MuMIn	Multi-Model Inference
N	Nitrogen
NMDS	Non-metric Multidimensional Scaling
NMR	Nuclear Magnetic Resonance
O	Oxygen
POM	Particulate Organic Matter
KBr	Potassium bromide
RMSE	Root Mean Square Error
SOC	Soil Organic Carbon

Persons involved

François Maillard (supervisor), Allison Gill (collaborator), Per Persson (collaborator) and Anders Tunlid (co-supervisor).

1 Introduction

Terrestrial ecosystems store large quantities of organic carbon (C), primarily in soils through organic matter (Schmidt et al., 2011; Buckeridge et al., 2022). In the current context of climate change largely caused by anthropogenic CO_2 emissions, maintaining and increasing the sequestration of C in soils is a key mitigation strategy linked with current climate change politics of mitigation (Lal, 2004). As such, understanding the formation of stable soil organic carbon (SOC) is critical not only for accurately predicting the C cycle in terrestrial ecosystems but also adapting and modifying agricultural as well as silvicultural practices to increase SOC stocks (Lal, 2016).

Soil organic matter can be separated into fractions based on the physicochemical properties of the organic molecules composing it. Mineral-associated organic matter (MAOM) consists of small molecular weight molecules adsorbed onto soil minerals, including clay minerals as well as iron and aluminum oxides (Figure 1). The mineral-adsorbed organic compounds are thus protected from microbial decomposition and can persist in soils for centuries (Cotrufo and Lavallee, 2022; Chen et al., 2024). The second fraction of organic matter in soils is called particulate organic matter (POM). This fraction is composed of insoluble molecules resistant to microbial decomposition, often long polymers that resist enzymatic attack, and persist in soils due to their recalcitrance or lack of energetic interest for microbial decomposers. The percentage of SOC stored either in MAOM or POM largely varies depending on soil types, land uses, and soil horizons, but POM-C is often dominant in the organic horizons while MAOM-C is more dominant in mineral horizons (Cotrufo and Lavallee, 2022; Chen et al., 2024).

Recent studies have challenged the belief that most SOC is primarily plant-derived, instead showing that a substantial fraction of SOC derives from microbial residues, particularly from mycelial dead residues or fungal necromass. For example, Liang et al. (2019) and Angst et al. (2021) highlight that fungal necromass-C can make up more than half of the stable SOC. There is also research which suggests that most of this fungal necromass-C was likely MAOM, with soluble fungal molecules adsorbing on minerals (see overview in Figure 1). Angst et al. (2021, 2024) found that a large fraction of POM-C is of fungal origin. This is unexpected, as fungal mycelium is not typically assumed to be composed of particular compounds highly resistant to microbial degradation. Indeed, in contrast to plant materials composed of lignocellulose, the fungal cell wall is mainly composed of mannoproteins, β-glucans, and chitin, which are more prone to degradation than lignin (Brethauer et al., 2020; Vega et al., 2012).

To study the decomposition dynamics of fungal necromass, scientists incubate in-vitro grown and killed mycelial biomass in mesh bags buried in soils, a method similar to that of studies on plant litter. Aligning with soil biogeochemistry results, studies using fungal necromass in mesh bags have found a substantial fraction of initial fungal necromass persisting, often ranging between 5 to 25% of the initial fungal necromass incubated in soils, depending on the studies of Brabcová et al. (2016); Beidler et al. (2020); Maillard et al. (2021); See et al. (2021). By producing and decomposing fungal necromass of different species with various biochemical compositions, scientists have found that this range of 5 to 25% of necromass mass remaining in mesh bags is best explained by variation in fungi biochemical composition at death. Specifically,

melanin, a pigment present in around 50% of soil fungi, likely contributes to the recalcitrance of melanized fungal necromass due to its aromatic structure, making it difficult to break down by soil microorganisms (Fernandez et al., 2019). This has been particularly well demonstrated using *Meliniomyces bicolor*, a fungal species where melanization can be induced depending on its growing culture, with melanized *M. bicolor* residues often presenting 20-30% of initial mass remaining at the end of the decomposition, while non-melanized *M. bicolor* necromass harbored only 8-12% of initial mass remaining at the end of the decomposition. Nevertheless, this also points out that even non-melanized mycelium presents a substantial fraction of its necromass as persistent POM post-death (Maillard et al., 2022, 2023b).

An often overlooked aspect of the fungal life cycle is the fact that fungal mycelium in soil can die at any physiological stage of development or age. This can be caused by a variety of biological and physical stressors, leading to a wide range of outcomes in mycelia physiological states at the time of death such as drought events, viral lysis, surrounding bacteria or fungi producing antibiotics (Sussman, 2013; Camenzind et al., 2023). Considering the death of mycelial biomass at different physiological states or ages, it can be assumed that young fungal biomass would possess more non-structural compounds of reserves like trehalose and glycogen, as well as proteins, making it a higher quality necromass that could be easily degradable by microbial decomposers (Thevelein, 1984; Fontana and Krisman, 1978). Fungal biomass of an intermediate age or having peaked in biomass production after having used available C and nutrients would start to be depleted in storage compounds and its necromass quality at death would be intermediate, mostly made of some structural compounds structuring the fungal cell wall like chitin and glucans (Vega et al., 2012). Finally, during a starvation phase, old fungal biomass would be fully depleted in labile compounds and in structural compounds that can be partially recycled, thus being of very low quality for microbial decomposers in soils. Collectively, this indicates that within a single fungal species, fungal biomass at death could likely vary drastically in biochemical composition and thus presenting contrasting decay dynamics in soils.

In this project, I aimed to test how the fungal physiological state at death affected the subsequent decomposition of the mycelial residues. To do so, I worked with a specific species of fungi, *Neurospora crassa*, a commonly found soil saprotrophic fungi that is not prone to melanization (Kuo et al., 2014; Turner et al., 2001). Similar to recent studies on necromass decomposition, I buried mesh bags filled with fungal necromass in soil and sequentially harvested them over time (See et al., 2021; Maillard et al., 2023b; Beidler et al., 2020)). I selected decomposition models from recent decay studies and calculated their corresponding decay parameters for our fungal necromass decomposition experiment (Gill et al., 2021; See et al., 2021). Additionally, to quantify the biochemical composition of the fungal necromass initially, and during decomposition, I used Diffuse Reflectance Infrared Fourier Transform Spectroscopy (DRIFTS) analysis. This allowed us to identify fungal compounds that were driving the decomposition process.

I hypothesized the following: (a) fungal biomass would gradually become more enriched in cell-wall compounds relative to non-structural compounds as the age of the fungus progressed; (b) linked with this previous assumption, I anticipated fungal necromass decay rates to decrease as fungal necromass age at death increased; and (c) I also hypothesized a larger fraction of fungal necromass would be resistant toward microbial decomposition and thus persist in soils as fungal necromass age at death increased.

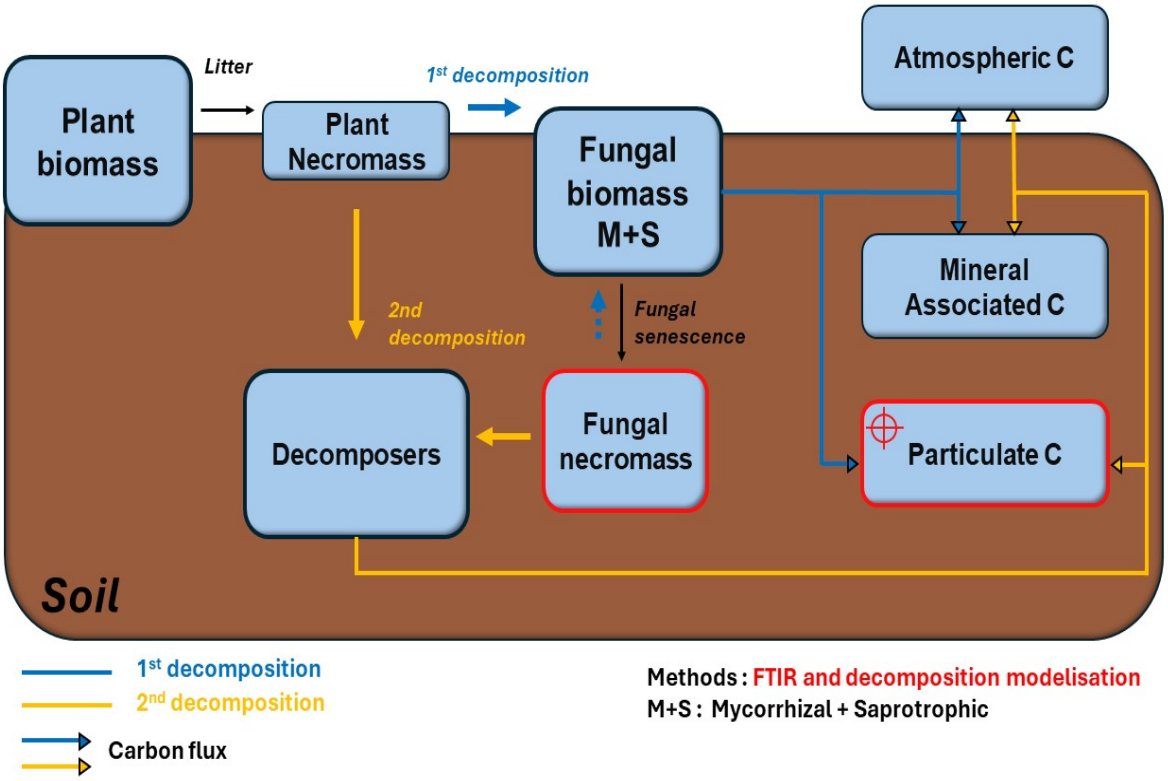

Figure 1: Overview of soil dynamics with a focus on carbon (C) fluxes. Colors differentiate between first and second decomposition pathways, arrows specify the decomposition-driven course of carbon flux. Colors surrounding boxes represent targeted methods used.

2 Background

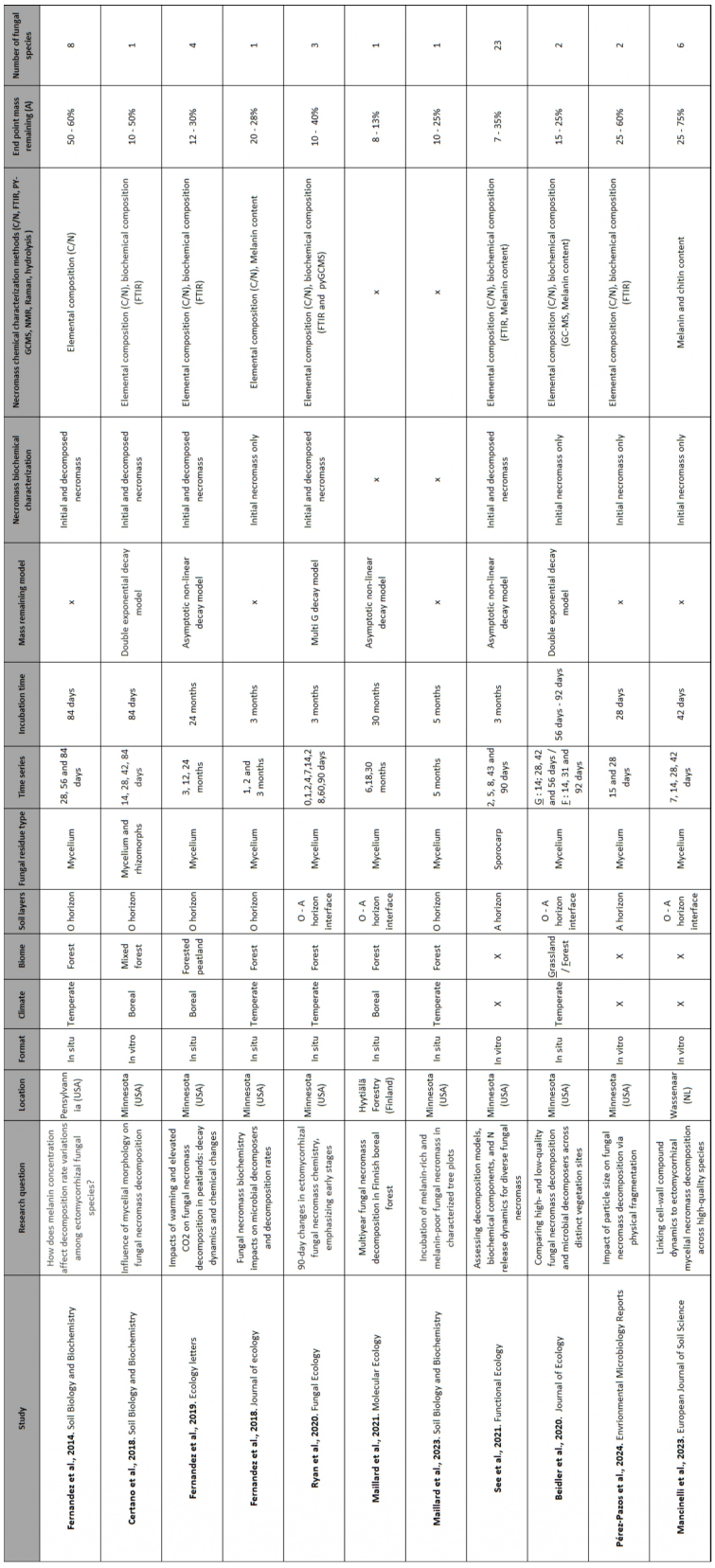

Study	Research question	Location	Format	Climate	Biome	Soil layers	Fungal residue type	Time series	Incubation time	Mass remaining model	Necromass biochemical characterization	Necromass chemical characterization methods (C/N, FTIR, PY-GCMS, NMR, Raman, hydrolysis)	End point mass remaining (A)	Number of fungal species
Fernandez et al., 2014. Soil Biology and Biochemistry	How does melanin concentration affect decomposition rate variations among ectomycorrhizal fungal species?	Pennsylvania (USA)	In situ	Temperate	Forest	O horizon	Mycelium	28, 56 and 84 days	84 days	x	Initial and decomposed necromass	Elemental composition (C/N)	50 - 60%	8
Cortano et al., 2018. Soil Biology and Biochemistry	Influence of mycelial morphology on fungal necromass decomposition	Minnesota (USA)	In vitro	Boreal	Mixed forest	O horizon	Mycelium and rhizomorphs	14, 28, 42, 84 days	84 days	Double exponential decay model	Initial and decomposed necromass	Elemental composition (C/N), biochemical composition (FTIR)	10 - 50%	1
Fernandez et al., 2019. Ecology letters	Impacts of warming and elevated CO2 on fungal necromass decomposition in peatlands: decay dynamics and chemical changes	Minnesota (USA)	In situ	Boreal	Forested peatland	O horizon	Mycelium	3, 12, 24 months	24 months	Asymptotic non-linear decay model	Initial and decomposed necromass	Elemental composition (C/N), biochemical composition (FTIR)	12 - 30%	4
Fernandez et al., 2018. Journal of ecology	Fungal necromass biochemistry impacts on microbial decomposers and decomposition rates	Minnesota (USA)	In situ	Temperate	Forest	O horizon	Mycelium	1, 2 and 3 months	3 months	x	Initial necromass only	Elemental composition (C/N), Melanin content	20 - 28%	1
Ryan et al., 2020. Fungal Ecology	90-day changes in ectomycorhizal fungal necromass chemistry, emphasizing early stages	Minnesota (USA)	In situ	Temperate	Forest	O - A horizon interface	Mycelium	0,1,2,4,7,14,2 8,60,90 days	3 months	Multi G decay model	Initial and decomposed necromass	Elemental composition (C/N), biochemical composition (FTIR and pyGCMS)	10 - 40%	3
Maillard et al., 2021. Molecular Ecology	Multiyear fungal necromass decomposition in Finnish boreal forest	Hyytiälä Forestry (Finland)	In situ	Boreal	Forest	O - A horizon interface	Mycelium	6,18,30 months	30 months	Asymptotic non-linear decay model	x	x	8 - 13%	1
Maillard et al., 2023. Soil Biology and Biochemistry	Incubation of melanin-rich and melanin-poor fungal necromass in characterized tree plots	Minnesota (USA)	In situ	Temperate	Forest	O horizon	Mycelium	5 months	5 months	x	x	x	10 - 25%	1
See et al., 2021. Functional Ecology	Assessing decomposition models, biochemical components, and N release dynamics for diverse fungal necromass	Minnesota (USA)	In vitro	X	X	A horizon	Sporocarp	2, 5, 8, 43 and 90 days	3 months	Asymptotic non-linear decay model	Initial and decomposed necromass	Elemental composition (C/N), biochemical composition (FTIR, Melanin content)	7 - 35%	23
Beidler et al., 2020. Journal of Ecology	Comparing high- and low-quality fungal necromass decomposition and microbial decomposers across distinct vegetation sites	Minnesota (USA)	In situ	Temperate	Grassland / forest	O - A horizon interface	Mycelium	G : 14; 28, 42 and 56 days / F : 14, 31 and 92 days	56 days - 92 days	Double exponential decay model	Initial necromass only	Elemental composition (C/N), biochemical composition (GC-MS, Melanin content)	15 - 25%	2
Pérez-Pazos et al., 2024. Environmental Microbiology Reports	Impact of particle size on fungal necromass decomposition via physical fragmentation	Minnesota (USA)	In vitro	X	X	A horizon	Mycelium	15 and 28 days	28 days	x	Initial necromass only	Elemental composition (C/N), biochemical composition (FTIR)	25 - 60%	2
Mancinelli et al., 2023. European Journal of Soil Science	Linking cell-wall compound dynamics to ectomycorrhizal mycelial necromass decomposition across high-quality species	Wassenaar (NL)	In vitro	X	X	O - A horizon interface	Mycelium	7, 14, 28, 42 days	42 days	x	Initial necromass only	Melanin and chitin content	25 - 75%	6

Figure 2: Comparison of selected studies on fungal necromass decomposition using buried mesh bags. "X" indicates a lack of information in a specific column.

2.1 Overview

Soil organic matter (SOM) is the largest terrestrial carbon (C) reservoir, storing more C than both vegetation and the atmosphere combined. Soil organic C (SOC) is the metric that directly relates to the C fluxes entering and leaving the soil, thereby playing a significant role in the global nutrient cycle (Liang et al., 2019). Fungal necromass, which consists of dead fungal residues, makes up a substantial fraction of soil organic C (ranging from 10 to 50%) (Liang et al., 2019)). Its degradation dynamics are directly linked to soil organic carbon (SOC) and soil organic matter (SOM). Studies have demonstrated that fungal necromass carbon (C) can account for more than half of the stable soil organic carbon (SOC). For example, Liang et al. (2019) and Angst et al. (2021) discovered that a significant fraction of SOC is composed of fungal necromass. Therefore, understanding its decomposition and stabilization in soils is crucial. This is surprising because fungal mycelium is not generally considered to contain compounds that are highly resistant to microbial degradation. Unlike plant materials composed of lignocellulose, fungal cell walls are mainly composed of mannoproteins, β-glucans, and chitin, which are more prone to degradation than lignin (Brethauer et al., 2020; Vega et al., 2012).

In summary, fungal necromass significantly contributes to stable SOC, despite its components being more susceptible to degradation compared to plant materials. This highlights the importance of fungal necromass in soil carbon dynamics and overall ecosystem functioning.

2.2 Fungal necromass production and mesh bag decomposition methods

To study the decomposition processes of fungal necromass, scientists often use nylon or polyester mesh bags with varying pore sizes filled with fungal residues. This tool standardizes the experimental setup and allows for the analysis of the remaining mass at any desired time point (Beidler et al., 2020). The fungal material placed in the mesh bags can be of various origins (i.e., different fungal species). Most studies use mycelium, which can easily be cultivated in the laboratory and then killed to create fungal necromass. Others, like See et al. (2021), might take samples directly from living organisms (sporocarps) in the field and then prepare the mesh bags similarly in the laboratory.

2.3 Study area

In terms of geographical representation, the focus is primarily on the northern hemisphere, with most studies conducted in temperate climates (Fernandez and Koide, 2014; Fernandez and Kennedy, 2018; Ryan et al., 2020; Maillard et al., 2023a; Beidler et al., 2020), followed by boreal climates (Certano et al., 2018; Fernandez et al., 2019; Maillard et al., 2021). Eight studies focus on forest biomes, two of them also addressing peatlands (Fernandez et al., 2019) and grasslands (Ryan et al., 2020). This provides insights and conclusions on fungal necromass decomposition primarily in temperate and boreal forests. This pattern of forest ecosystems being mostly studied for fungal necromass decomposition does not seem to be dedicated by any ecological relevance as fungi represent an abundant microbial group in most terrestrial ecosystems, but rather reflects the fact that this research field is relatively new and dominated by a few research groups that primarily study forest ecosystems. I anticipate that in the future, more fungal necromass decomposition studies using mesh bags will be conducted in tropical and boreal biomes.

Regarding the representation of studies, three of them examined necromass decomposition in an in vitro environment, which limits observations related to soil origin (See et al., 2021; Pérez-Pazos et al., 2024; Mancinelli et al., 2023). However, it is important to note these studies were not focused on comparing biome or soil types together but rather focused on fungal residue chemical differences (See et al., 2021; Mancinelli et al., 2023); or on the effect of different fungal necromass decomposers (Pérez-Pazos et al., 2024).

2.4 Soil profile and fungal necromass

The studies by Fernandez and Koide (2014); Fernandez and Kennedy (2018); Fernandez et al. (2019); Certano et al. (2018); Maillard et al. (2023a) all buried their fungal decomposition mesh-bags on the O horizon. In contrast, See et al. (2021) and Pérez-Pazos et al. (2024) focused on the A horizon. The rest of the studies chose to use a depth at the interface of O and A horizon. These depth differences would most likely impact the resulting mass remaining fungal residues in buried bags. While the incubation horizon for fungal necromass is not often justified in the aforementioned studies; O horizon and topsoil layers have been chosen as fungal biomass is high in these soil layers, and thus the production of natural "necromass" is also high. Now regarding the relative contribution of plant and fungal C in soil organic C stocks, deep soil layers rather than topsoil would like be more dominated by fungal necromass-C than plant necromass-C. Consequently, it would be interesting to study the decomposition of fungal necromass in deep soil layers to inform global C cycle.

2.5 Fungal necromass type

In terrestrial ecosystems, fungi can occur both as mycelium in soils as well as fruit bodies (their reproductive structures). Thus, both fungal mycelium and fruit bodies represent sources of fungal necromass. The studies by Fernandez and Koide (2014); Fernandez and Kennedy (2018); Fernandez et al. (2019), Certano et al. (2018), Maillard et al. (2021, 2023a), Ryan et al. (2020), and Beidler et al. (2020) all focus on mycelium. However, some studies also examine other types of fungal residue, such as rhizomorphs (Certano et al., 2018). Only See et al. (2021) explored the decomposition of fruiting bodies. Yet, it is very likely that both fungal necromass types, either mycelial or fruit bodies, experience different decay pathways. For example, mycelium is often microscopic and often sturdy limiting it is grazing by fauna, while fruit bodies of a large set of fungi is edible for wildlife and rapidly ingested by fauna.

2.6 Experimental design

In terms of time series, some studies have only one or two time points, while others have multiple time points over the course of the incubation period. For example, the study by Ryan et al. (2020) has 9 time points over 90 days, while the study by Fernandez and Kennedy (2018) has only 3 time points over 3 months. The frequency and duration of sampling can affect the results of decomposition studies. Shorter incubation times and fewer time points may not capture the full extent of decomposition, while longer incubation times and more frequent sampling can provide more detailed information on decomposition dynamics. However, only 3 studies Fernandez et al. (2019); Maillard et al. (2021, 2023a) exceed the amount of 3 months of incubation time, and they have a maximum of 3 time series. On the other hand, Ryan et al. (2020) has only a 3-month

incubation time, but they have the highest capacity to grasp the full extent of decomposition with 9 time series.

2.7 Decomposition data through modelling

The accuracy of decomposition studies depends on having a sufficient number of time series with a long enough decomposition period. The variability in these parameters among the studies may explain the differences in the best-fit models chosen. Among the studies that conducted a best-fit analysis, three found the asymptotic decay model to be the best choice (Fernandez et al., 2019; Maillard et al., 2021; See et al., 2021), while Certano et al. (2018) and Beidler et al. (2020) found the double asymptotic model to be more appropriate. Ryan et al. (2020) opted for a more complex representation using a Multi-G decay model. It is worth noting that both the double and asymptotic models represent decomposition from a "two-pool" perspective and can be used on smaller datasets while still providing meaningful results. In contrast, the Multi-G decay model used by Ryan et al. (2020) is more complex and requires a larger dataset to be effective, which is reflected in the fact that this study had the most time series.

2.8 Chemical composition analysis method

Studies that conducted chemical composition analysis had different approaches for selecting which time series of necromass to quantify chemically. Five of them performed chemical composition analysis before the decomposition experiment and throughout it to assess chemical changes and link them with decomposition results (Fernandez and Koide, 2014; Certano et al., 2018; Fernandez et al., 2019; Ryan et al., 2020; See et al., 2021). In contrast, the rest of the studies chose to only characterize the necromass prior to the decomposition process, also known as initial necromass (Fernandez and Kennedy, 2018; Beidler et al., 2020; Pérez-Pazos et al., 2024; Mancinelli et al., 2023). Scientists want to characterize the chemical compounds of fungal necromass to then link them with decomposition decay trajectories. Typically, some compounds present in the fungal cell wall, like melanin, prove to be resilient to microbial degradation in the soil, hence resulting in slower decomposition. Alternatively, intracellular compounds like nitrogen are considered higher-quality substrates for microbial degradation, hence leading to faster decomposition rates in the soil (Ryan et al., 2020). The studies also differed in the techniques selected for chemical characterization. However, they were homogeneous in using elemental composition (C/N), except for Mancinelli et al. (2023), which mainly focused on melanin and chitin content. Elemental composition (C/N) was usually coupled with the biochemical composition FTIR technique (Certano et al., 2018; Fernandez et al., 2019; Ryan et al., 2020; See et al., 2021; Pérez-Pazos et al., 2024). Additionally, other approaches were used to analyze chemical composition, such as pyGCMS (Ryan et al., 2020), GC-MS (Beidler et al., 2020), and chitin content (Mancinelli et al., 2023). Overall, the techniques used likely depend on the research questions and the specific characteristics that the necromass studied might have (such as melanin).

2.9 Fungal species and biochemical compounds linked with decomposition dynamics

Numerous studies have compared the decomposition dynamics of different fungal species, highlighting the significance of biochemical composition and decay trajectories. Fernandez and Koide (2014) demonstrated that fungal tissues with high melanin and low nitrogen content decay more slowly than those with low melanin and high nitrogen content, indicating that necromass quality influences decomposition rates. This finding was corroborated by Fernandez et al. (2019), who showed that initial nitrogen content predicted early decay rates, while melanin content determined mass remaining after two years, using an asymptotic non-linear decay model. Similarly, Ryan et al. (2020) found that both melanin and nitrogen content were crucial in controlling decomposition rates, with high nitrogen content accelerating decomposition when melanin content was insufficient. Several studies have focused on a single species to eliminate confounding factors introduced by multiple species. Certano et al. (2018) examined *Armillaria mellea*, employing a double exponential decay model, and found that initial nitrogen concentration positively correlated with mass loss. Fernandez and Kennedy (2018) used *Meliniomyces bicolor*, a species with variable melanin content, to confirm the independent effects of melanin and nitrogen on subsequent decomposition. Other research has explored a broader range of species. See et al. (2021) investigated a pool of 23 species, proposing a two-pool model of necromass decomposition with distinct biochemical fractions. Mancinelli et al. (2023) studied six ectomycorrhizal fungal species and found that, despite similar overall mass loss during decomposition, each species affected soil organic matter differently due to unique patterns of cell-wall compound loss. These studies collectively underscore the importance of biochemical composition, particularly melanin and nitrogen content, in governing fungal necromass decomposition. They also highlight the variability in decay trajectories, with different models employed to describe these processes. The findings provide valuable insights for incorporating fungal necromass into biogeochemical models and understanding nutrient cycling in soil ecosystems.

2.10 Decomposition results

For end point mass remaining (A), the values range from as low as 7% to as high as 75% (See et al., 2021; Mancinelli et al., 2023). Fernandez and Koide (2014) reported a relatively high-end point mass remaining of 50-60%, while Maillard et al. (2021) reported a much lower value of 8-13%. The other studies fall within this range, with values ranging from 10-25% to 25-60%.

2.11 Summary

Soil organic matter (SOM) is the largest terrestrial carbon reservoir, and fungal necromass plays a crucial role in carbon sequestration, despite its components being more susceptible to degradation compared to plant materials. Studies using mesh bags to investigate fungal necromass decomposition have primarily focused on temperate and boreal climates, particularly in forest biomes. These studies highlight the importance of biochemical composition, especially melanin and nitrogen content, in governing decomposition rates and trajectories. Different experimental designs, including variations in incubation depth, time series, and chemical analysis methods, have been employed, leading to the use of various decay models. Future research should expand to tropical and boreal biomes, explore the decomposition dynamics of fungal

necromass in deep soil layers, and encompass longer decomposition times to better describe the fungal decay dynamic.

3 Methods

3.1 Fungal Necromass Production

To investigate how the fungal physiological state at death affect the subsequent decomposition of the fungal necromass, the fungal species selected was *Neurospora crassa*. I chose this *N. crassa* primarily due to its fast growth rate in vitro, allowing for efficient production of biomass. *N. crassa* was also a pertinent choice from an ecological perspective, since it is found in a broad range of ecosystems such as tropical, subtropical, and boreal (Kuo et al., 2014; Turner et al., 2001). Additionally, *N. crassa* is also part of one of the soil's most abundant fungal classes, the Sordariomycetes from the Ascomycota division (Blaschke et al., 2023). These geographical and phylogenetical characteristics allowed the use of *N. crassa* as a representative species to study the decomposition of mycelial residues in soils.

N. crassa was cultivated in 250 ml flasks filled with 150 ml of liquid potato-dextrose medium at half-strength, a typical medium for fungal growth. Flasks were agitated at 100 rpm on an orbital shaker at 20°C, and finally, the biomass was harvested and killed at seven successive incubations times (following being 2, 4, 8, 15, 29, 46 and 67 days, as shown in Figure 3). By doing so, I obtained seven different physiological state at death. Figure 3 summarizes all seven time points collected (days) and mentions their weighted biomass (g/L). The development in biomass of *N. crassa* displayed three distinct tendencies. First, steady growth was noticeable from day 2 until day 8, with a relatively young biomass going from $0.2g/L$ to $2.6g/L$. Then, from the intermediate range of 15 to 29 days, some mass was definitively lost, going from $3.4g/L$ to $2g/L$ which represented a 41% mass loss. From 29 to 67 days, there was still a mass loss, but it appeared to be more stabilized, with around 15% mass loss over a longer time range. These three distinct trends could already be preliminary linked to our hypothesis suggestion around biochemical composition at various ages.

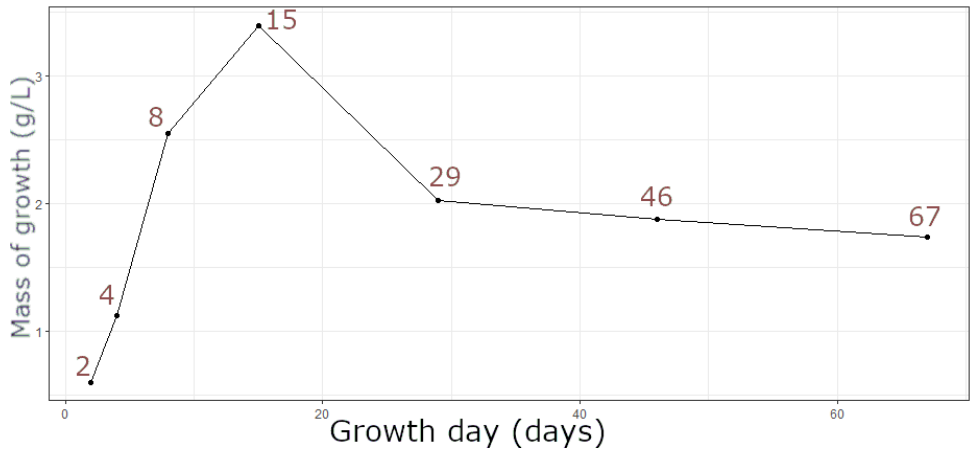

Figure 3: Biomass production for the necromass decomposition experiment. Numbers in dark red represented the specific number of growth days before collection.

The collected fungal biomass was rinsed with distilled water on a sieve in order to remove any trace of the growth medium. It was then homogenized and frozen at -80°C, which ensured the death of the mycelium. The resulting fungal biomass was then freeze-dried. The final product of this process was considered as dead mycelial residues, also called fungal necromass. I then prepared mesh-bags, or "mycobags", with a dimension of 5 x 10 cm, filled with 50 mg of fungal necromass before being sealed. The bags had a 43 µm mesh size that allowed the exclusion of tree roots inside and excludes soil particle penetration. This allowed reliable quantification of fungal necromass degradation rates (Beidler et al., 2020). The current necromass production section, the following experiments and analysis sections were summarized in Figure 4.

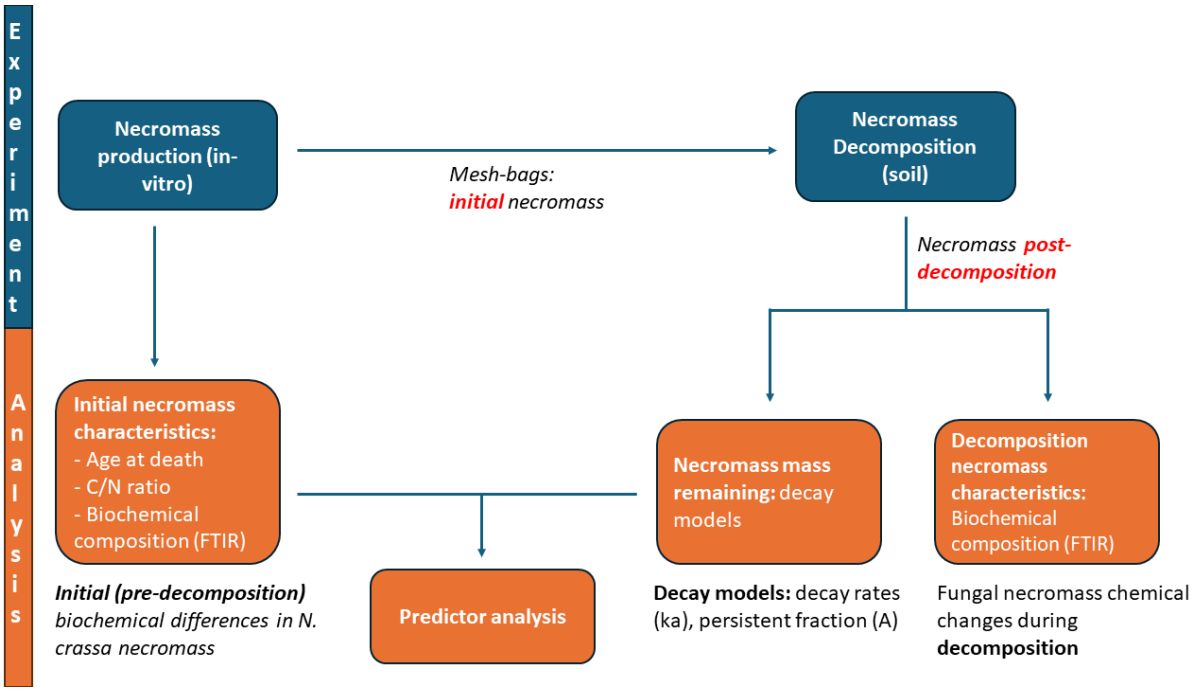

Figure 4: Overview of the experiment and analysis workflow. "Initial" and "decomposition" were written as bold to emphasize the different biochemical state between these two and to what analysis they were inherently linked.

3.2 Fungal Necromass Decomposition in Soils

I buried the mycobags in the topsoil of a 60-year-old Spruce (*Picea abies*) forest at Lund University's Stensoffa field station (55.6951° N, 13.4472° E). I selected a Spruce plantation as these forests hold significant economic interest in Sweden, and a deeper understanding of their soil C and nutrient cycles linked to the decomposition of fungal necromass could greatly impact wood-production potential while maintaining soil C sequestration potential (Jandl et al., 2007). 175 mesh bags were buried in the topsoil of the selected study area. Each mycobag contained 50 mg dry mass of a specific necromass age (2 , 4, 8, 15, 29, 46 and 67 days, as described in *2.1 Fungal Necromass Production*). Those 175 mesh bags were divided into 5 randomly chosen plots within the forest site, with 35 mesh bags per plot. Each plot carried the same experiment design, which means that they were replicates. Additionally, each plot held 5 mycobags per necromass age (5 mycobags x 7 necromass age). The mycobags were then collected at different decompositions stages during summer and fall of 2023 (at days 10, 20, 40, 76 and 117, as shown in Figure 1). This translated into 5 different times of decomposition for each necromass age.

In other words, once the experiment was established, mycobags were collected on the days of decomposition presented in Table 1. As for equipment, a small shovel and field flags were used to bury and later localize the different samples and plots prepared. Once collected, the mycobags were brought back to the lab, opened, and the decomposed necromass was carefully removed to avoid contamination of the fungal dead residues with surrounding soil particles. It was then transferred into 1.5 ml tubes, frozen at -80°C, and freeze-dried for subsequent analysis. The experiment started on July 7th, 2023 and ended on November 1st, 2023.

Table 1: Summary of our main potential drivers of decomposition.

Drivers of decomposition	Values
Necromass age (*day*)	[2, 4, 8, 15, 29, 46, 67]
Decomposition times (*day*)	[10, 20, 40, 76, 117]

Regarding our data analysis based on the collection of samples in the field, certain abnormal weather conditions were worth mentioning. Our field campaign started on July 7th 2023 and ended on November 1st 2023, which coincided with a dry spell that took place mainly in southern Sweden, where our own experiment took place. Additionally, our experimental sites were subjected to disturbance by local wildlife (birds, mammals). I found some of our mycobags detached from their initial location and left nearby on the soil surface. This, combined with meteorological disturbance, could explain some suprising mass remaining values sampled (as shown in Figure 5, in the result section), increasing values in the latter stage of decomposition, despite an overall decreasing mass loss trend.

3.3 Fungal Decay Parameters Modeling

3.3.1 Approach and Model Selection

Once the entire field campaign was completed, the data from the weighted mycobags provided us with a dataset to fit models on (as shown in the overview analysis in Figure 4). Our field experiment dataset presented rates of decomposition between time point 0 and time point 117 days for each necromass age (as shown in Figure 5). For this part of the analysis, I chose to work with two different models, using Gill et al. (2021) decomposition study on plant litter as a template. The following models were described in the Table 2. Fungal residue decay being a new field of research, I chose to transpose analysis methods from the more established study area of plant litter decomposition (Gill et al., 2021), into our fungal necromass decomposition. I therefore used the same decay models, adjusting model parameters to our necromass decomposition setup. Additionally, our model selection was based on an index of accuracy (Root Mean Square Error, *RMSE*, Chai and Draxler,2014) with a secondary approach to complexity (Akaike Information Criterion, AIC_c,Burnham and Anderson, 2002). Models could then be linked with ecological outcomes, for example single exponential model represented a decomposition pattern with a steady decay rate, or "k". This would mean that the entire pool of compounds present in the necromass would decompose in the same manner, as in, at the same speed, and entirely. Further, I increased mathematical complexity with an asymptotic model, which led us to explore scenarios with multiple decay rates. Concerning the asymptotic model, two decomposition pools are effective, one representing a pool with a faster decomposition rate and a second representing

a slower decomposition rate. This is interesting since I wanted to have an overview on which compounds, or in a broader scale, which pools of compounds might be linked with the eventual recalcitrance of our fungal necromass.

Table 2: Model representation with their corresponding formula and references.

Model	Formula	References
Single exponential	$X = e^{-k_s \cdot t}$	(Olson, 1963)
Asymptotic	$X = A + (1 - A) \cdot e^{-k_a \cdot t}$	(Hobbie, 2008)

3.3.2 Model Formulas

The models differed in complexity, and their formulas addressed the decomposition rates of the data in different manners. For example, the single exponential model used a single decomposition constant (k_s) to describe the necromass mass remaining (X), and time of decomposition (t). The asymptotic model formula, however, brought a more complex approach of two decay rates. The first one represented a "fast pool" of decay that decomposed at a rate of k_a. The second rate stood for a "slow pool" with a near-zero decay value, represented by a plateau in the decomposition process, and labelled as asymptote A (Gill et al., 2021). By linking this two-pool perspective to our biochemical composition introduction hypothesis, I could assess the hypothesis that the faster pool was composed mainly of labile compounds, while the more recalcitrant one was harder to degrade.

3.3.3 Parameters Selection

The best fit approach was carried out with RStudio Team (2024), using the programming script that Gill et al. (2021) used in their plant litter experiment as a template. The modeling collaboration with the main author began at this point, particularly to receive feedback on how to adapt Gill et al. (2021) model into our necromass decomposition experiment. Parameters were selected through an analysis on Geogebra (2024) where formulas were plotted and linked with our mass loss data analysis (as shown in Figure 5). Five values were selected per model (as shown in Table 3), and these parameter value range were chosen to reflect the lower and higher extremes of the decay rates I were analyzing. The aim was to allow a range of parameters that could explain the data while still providing enough variability in the analysis to reach convergence.

Table 3: Parameter values selected for the model best fit approach on RStudio Team (2024)

Model	Parameter	Value 1	Value 2	Value 3	Value 4	Value 5
Single exponential	k_s (day^{-1})	0.1	0.5	1	1.5	2.5
Asymptotic	A (% remaining fraction)	0.8	0.631	0.463	0.294	0.125
	k_a (day^{-1})	0.08	0.089	0.0978	0.106	0.115

3.3.4 Root Mean Square Error and Akaike Information Criterion

From the analysis through the programming code script in RStudio Team (2024), I gathered the results of the parameter best fit and their corresponding *RMSE* as well as AIC_c. Both were useful in considering how well of a fit our selected models were. AIC_c for example, was useful for measuring the complexity of a studied model (Burnham and Anderson, 2002). When looking at accuracy, or model performance, *RMSE* was a better selection criteria, as it informed differences between the decomposition field experiment values and the values calculated from the model analysis (Hodson, 2022).

3.4 Fungal Necromass Biochemical Composition

To determine the biochemical composition of both initial (as shown in fungal necromass production section) and decomposed fungal necromass, I used Diffuse Reflectance Fourier Transform Spectroscopy (DRIFTS, as shown in the overview analysis in Figure 4). DRIFTS allowed for relatively rapid analysis of the biochemical composition of organic samples by interpreting infrared beam absorption profiles in the mid-infrared region, which correspond to molecular functional groups (C-C, C-O, N-H bonds, etc.). This analysis linked observed wavelength peaks with regions of the selected spectrum previously characterized in the literature (as shown in Table 4, (Maillard et al., 2023b; Cocozza et al., 2003; Niemeyer et al., 1992)).

Moreover, DRIFTS enabled the chemical characterization of samples of only a few milligrams following dilution in Potassium bromide (*KBr*). This was crucial given the often-rapid decomposition of fungal necromass in soils and the relatively low fungal necromass mass remaining during decomposition, which would not have been easily done with techniques requiring a larger sample mass, such as Nuclear Magnetic Resonance (NMR) spectroscopy and pyrolysis Gas Chromatography-Mass Spectrometry (GC-MS).

Further, each necromass sample was mixed with *KBr* at a 1% mass/mass ratio (meaning that for each sample, I used 3mg of necromass for 297 mg of *KBr*) and analyzed by DRIFTS on a Fourier Transform Infrared Spectroscopy (FTIR) spectrometer (Bruker Vertex 80 v, Ettlingen, Germany) in a temperature-controlled room at 21 °C. 184 scans were averaged across the 3800 - 400 cm^{-1} range at a resolution of 4 cm^{-1}. Background subtraction was performed using a pure *KBr* spectrum (300mg *KBr*), and a baseline correction was used to eliminate baseline distortions. Both background subtraction and baseline correction were carried out in OPUS software (Bruker Corporation, 2023), and peak heights were normalized by calculating z-scores on Microsoft Excel (Microsoft Corporation, 2023). Wavelength peaks were identified based on the literature on the biochemical composition of fungal biomass and necromass and separated into functional groups (aliphatics, polysaccharides, amides, and aromatic compounds, as shown in Table 4, see end of *2. Method*) (Certano et al., 2018; Maillard et al., 2023b; Ryan et al., 2020; See et al., 2021). Peaks that lacked a clear identification based on literature, or were ambiguous, were labeled as "Unclassified" but were still included in the statistical analysis alongside the identified peaks. Given that FTIR only allowed relative abundance quantification, functional groups intensities were interpreted as concentrations. Total carbon (C) and nitrogen (N) contents were quantified from 3 mg of the fungal necromass. These analyses were conducted by the SilvaTech platform (INRAE, France) using a CHN analyzer (Carlo Erba NA1500, Italy). I then calculated the C/N ratio of the fungal necromass prior to incubation in soil. C/N has often been used as an indicator

for plant residue quality, with high C/N ratio indicating low residue quality and thus slower decay rates, and higher remaining mass fraction (Ostrowska and Porębska, 2015).

3.5 Multi-model Inference on Predictor Analysis Asymptote "A" and Decay Rate "ka"

Multi-model inference analysis was conducted from the RStudio Team (2024) package "MuMIn" to determine potential predictors of fungal necromass decay dynamics. This was conducted by comparing fungal necromass initial parameters (fungal biomass age at death, C/N ratio, FTIR functional groups) with decay model parameters (decay rate k_a and asymptote A). By using model selection and averaging, I obtained Fisher statistics p-values and an attributed weight value per variable.

3.6 Statistical Analysis on Initial Necromass Characteristics and Necromass Decay Models

An analysis of variance (One way ANOVA, Kim (2017)) was conducted on the asymptotic model parameters (k_a, A), as well as the initial biochemical composition (FTIR), followed by a post hoc Tukey's test. The reason of these statistic choices was to determine if there was any significant difference between the means. After conducting the ANOVA, the p-values were significant, allowing the follow up of the analysis with establishing which groups differed from each other using Tukey's honestly significance difference statistical test (Abdi and Williams, 2010).

Table 4: Wavelength peak annotation with compounds assessment from the literature (Maillard et al., 2023b; Cocozza et al., 2003; Niemeyer et al., 1992). The "Unclassified" mention represented peaks that could not be assigned through literature, either because of a lack of information, or ambiguity.

Wavelengths	Functional group	Potential compound
2926.93	$C-H$	Aliphatic
2857.91	$C-H$	Aliphatic
1660.29	$N-H$	Amide
1537.28	$C=O$	Amide
1453.46	$C-H$	Unclassified
1416.98	$C=C$	Aromatic
1393.67	$C-H$	Unclassified
1371.98	$C-H$	Unclassified
1315.09	$C-H$	Unclassified
1247.86	$C=C$	Aromatic
1202.46	$C-O$	Unclassified
1148.99	$C-O$	Unclassified
1075.81	$C-O$	Polysaccharide
1039.31	$C-O$	Polysaccharide
927.69	$=C-H$	Unclassified
894.67	$C-O$	Unclassified
853.20	$C-H$	Aromatic
853.20	Unclassified	Unclassified
822.03	Unclassified	Unclassified
802.58	Unclassified	Unclassified
759.43	Unclassified	Unclassified
704.71	$C-H$	Aromatic
632.39	Unclassified	Unclassified
608.69	Unclassified	Unclassified
571.91	Unclassified	Unclassified
532.10	Unclassified	Unclassified
470.39	Unclassified	Unclassified
436.64	Unclassified	Unclassified
427.82	Unclassified	Unclassified
409.23	Unclassified	Unclassified

4 Results

4.1 Necromass Decomposition

4.1.1 Decomposition Data

To analyze the effect of fungal necromass age, or physiological state at death, on the decomposition dynamics of *N. crassa* necromass decomposed in forest soils, I plotted the percentage of necromass mass remaining (dry mass relative to initial) depending on the necromass ages and decomposition times in soils (as described in figure 5).

Regardless of necromass ages, I observed a first phase of rapid fungal necromass mass loss within the first 20 days, followed by a plateau phase. However, these general trends were largely influenced by the ages of necromass, with young fungal necromass at death reaching a plateau phase in terms of mass loss sooner than older residues. For example, necromass ages 2 and 4 plateaued in mass remaining fraction after 40 days of decomposition, while necromass ages 8 and 15 plateaued after 65 days of decomposition instead. Older necromass ages of 29, 46 and 67 did not clearly plateau by the last decomposition measurement. Additionally, I noticed a strong effect of necromass age on the quantity of mass remaining at the end of the decomposition, with necromass ages 2 and 4 around 8% mass remaining fraction at the end of the experiment. Compared to that, necromass ages 46 to 67 ranged around 50 % mass remaining fraction. Overall, our results showed that fungal necromass age at death ("necromass age"), was a key driver in the decomposition dynamics of the mycelial residues in soils.

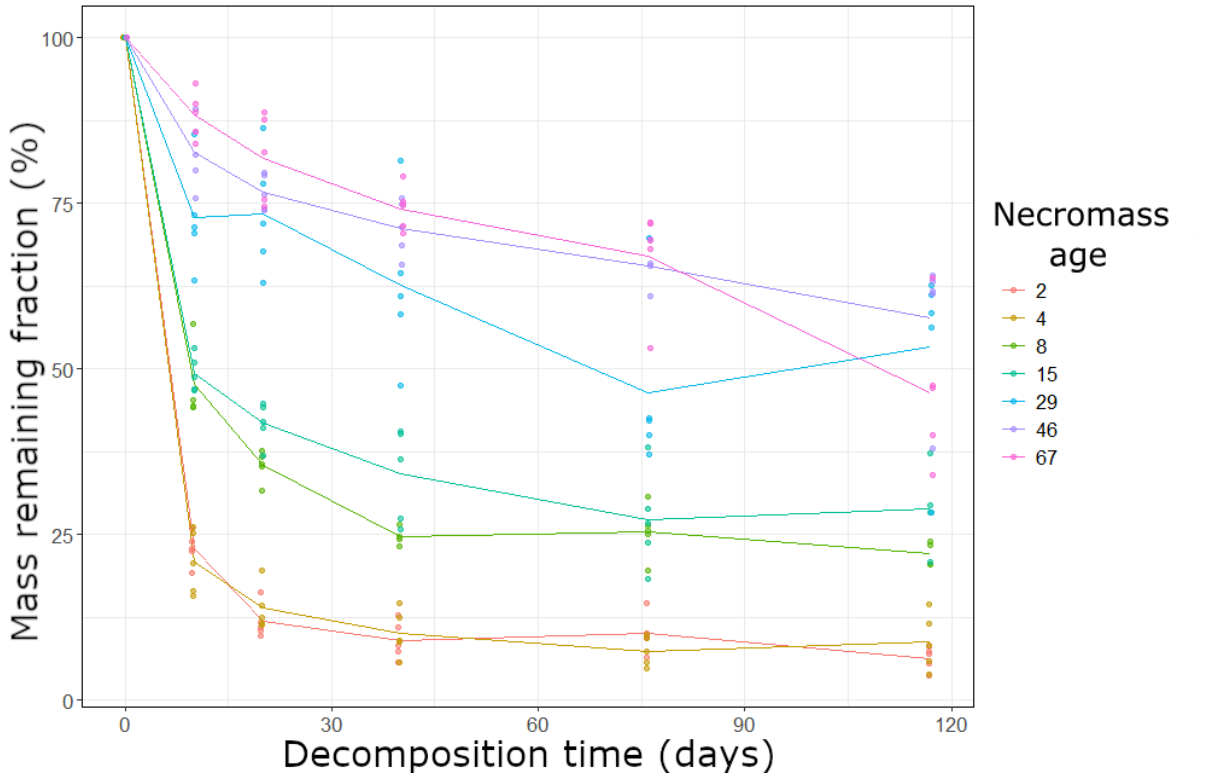

Figure 5: Percent of fungal necromass mass remaining depending on decomposition time (in days) and on fungal necromass age at death (in days, n=5 per decomposition time per necromass type).

4.1.2 Decomposition Models

To analyse what was the best mathematical fit, or what formulas (mathematical models) captured the complexity of the fungal necromass decomposition rates measured and illustrated in Figure 5, I ran a model comparison of asymptotic versus single exponential based on our selection of parameters, looked at *RMSE* as our main selection filter and considered AIC_c when two models were on a tie (see Table 5). Concerning the entire analysis, the simple exponential model was always superseded by the asymptotic model, the latter being then the best candidate (as shown in Table 6). However, despite our main selection criteria (*RMSE*) consistently favouring the asymptotic model, some AIC_c values also favoured the single exponential model in necromass ages 2 and 67, indicating momentarily less complexity for the single model. This observation on AIC_c values could be linked to *RMSE* values between models fits being extremely close for necromass ages 2 and 67 (N_2 δ : 0.012 and N_{67} δ : 0.004). Additionally, these close δ in *RMSE* could be observed in Figure 6, in (a) and (b), where the asymptotic and single exponential model representation were plotted very close to each other, hence the low resulting δ in *RMSE*. (c) displayed a situation where the single exponential model was imprecise fitting data points of the decomposition field data, hence the higher value (less precise) in the δ of *RMSE* for necromass age 67, which can be applied for necromass age 2 as well. Overall, despite a few situations where it was interesting to note that the simple exponential model approached the accuracy of the asymptotic model, the asymptotic model remained the best-fit model.

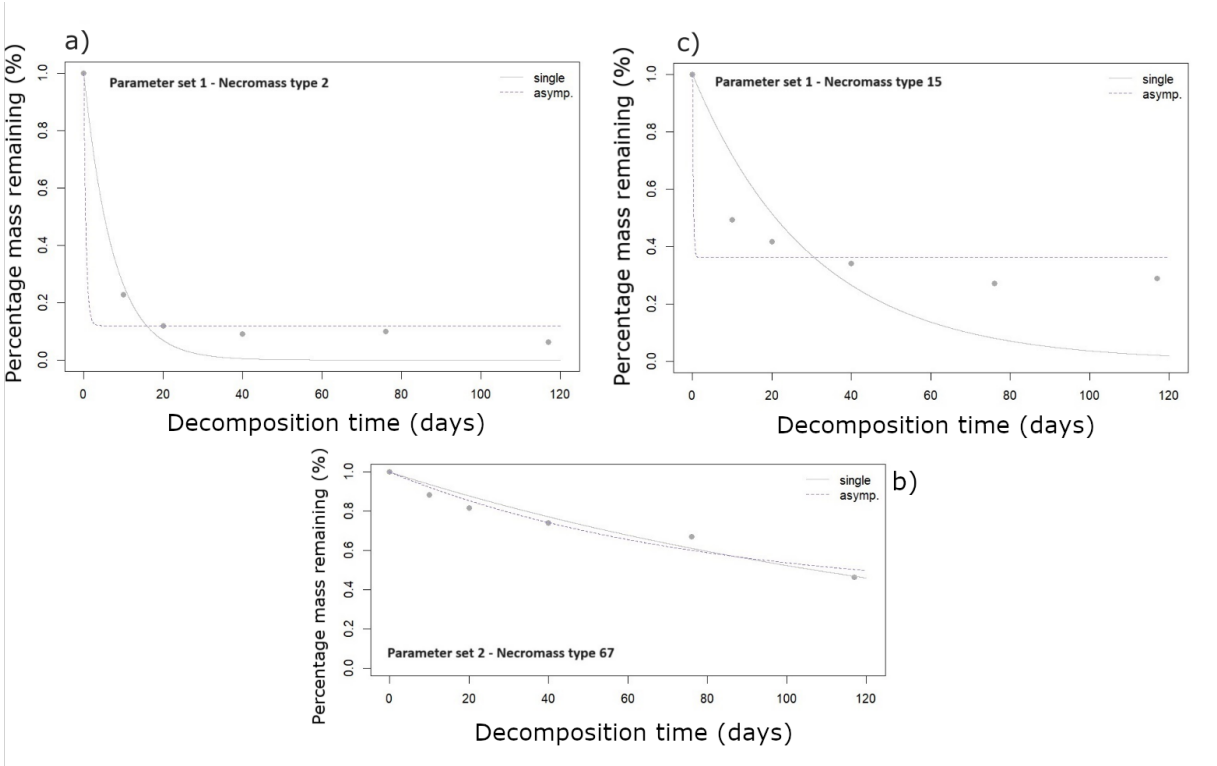

Figure 6: Effect of different modeling best fit on specific necromass decomposition. (a) concerned necromass age 2 using the parameter set 1 and (b) concerned necromass age 67 using the parameter set 2, these two situation represented a scenario where the fit between model was very close. (c) concerned necromass age 15 using the parameter set 1, which instead, represented a situation where the best fit was more evident.

Table 5: Results values from model decomposition best fit analysis with single exponential and asymptotic models. Bold values referred to the lowest value of RMSE and AIC_c, according to the selected necromass age.

	Single exponential			Asymptotic model			
Necromass age	k_s	AIC_c	*RMSE*	k_a	A	AIC_c	*RMSE*
2	0.134	**-12.915**	0.064	26.051	0.120	-10.405	**0.052**
4	0.138	-11.749	0.071	26.448	0.122	**-12.411**	**0.044**
8	0.048	-2.962	0.147	0.110	0.241	**-23.978**	**0.017**
15	0.033	-1.205	0.170	0.115	0.304	**-17.451**	**0.029**
29	0.009	-5.449	0.120	0.05	0.512	**-11.198**	**0.049**
46	0.006	-9.988	0.082	0.044	0.614	**-17.804**	**0.028**
67	0.006	**-17.860**	0.043	0.013	0.362	-13.980	**0.039**

Table 6: Summary of the best model selection per necromass age. This selection is based on RMSE filtering.

Necromass age	Best model fit
2	Asymptotic
4	Asymptotic
8	Asymptotic
15	Asymptotic
29	Asymptotic
46	Asymptotic
67	Asymptotic

4.1.3 Asymptotic Model Parameters

Once the asymptotic model was selected, I plotted its final parameter values (A,k_a) for each necromass age, this was done to determine the physiological state of *N. crassa* necromass at death driver (as shown in Figure 7). Both parameters seemed to be affected by the age of the necromass. A, the remaining fungal necromass fraction with a decomposing rate of 0, increased from necromass age 2 until 46, and then decreased for necromass age 67. k_a or the decomposition rate, displayed a high decay rate value for necromass age 2, and then gradually slowed down its rate of decomposition through the other necromass ages. This meant that the decomposition rate, especially for "younger" necromass age (from age 2 to 8), was relatively fast, until it decreased to slower rates of decomposition for "older" necromass age (past age 15). However, this pattern did not translate into a linear relationship for A, the remaining mass fraction, which peaked at necromass age 46 and decreased for necromass age 67. Additionally, it was then surprising that necromass age 67 had the slowest decomposition rate but a lower A than 46 or 29. Overall, these results closely followed the decomposition data of the field experiment seen in Figure 5, which brought further evidence that the asymptotic model is a suitable model to describe our decomposition experiment.

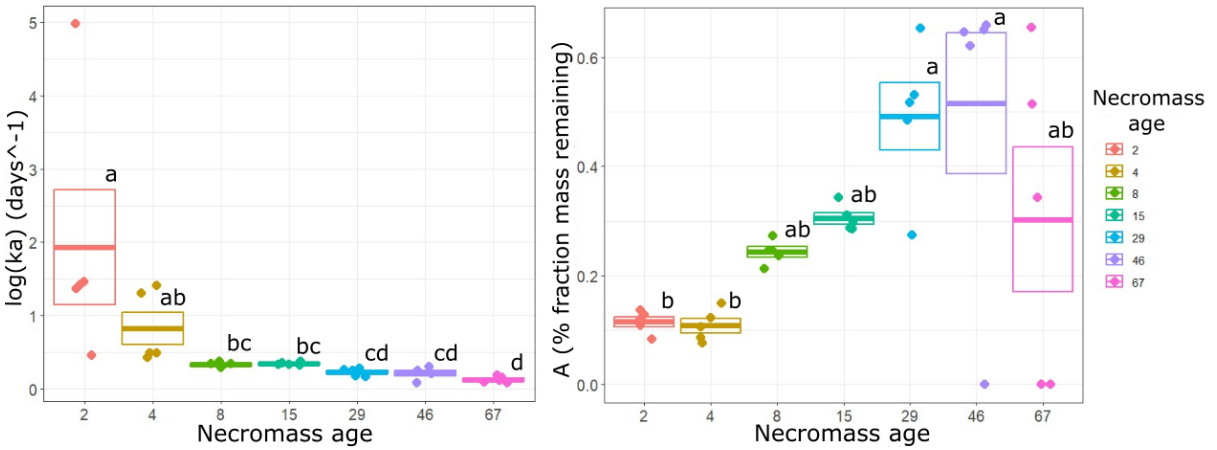

Figure 7: Asymptote (A) and decay rate (k_a) parameters values from the asymptotic model, plotted per necromass age (days). Letters a, b, c, and further combination represented results from the post hoc Tukey's test. Preliminary to the post hoc Tukey's test, a one-way ANOVA test was done on A and k_a, separately. The p-values were respectively $p_{\leq 0.01}$ and $p_{\leq 0.001}$.

4.2 Initial Necromass Biochemical Composition

4.2.1 Non Metric Multidimensional Scaling Analysis

I analyzed biochemical composition of the *N. crassa* necromass before decomposition in soils based on FTIR analysing using Non-metric Multidimensional Scaling (NMDS) followed by permutational multivariate analysis of variance (PERMANOVA) analysis using the intensity of peaks listed in Table 4. I plotted the data of our initial necromass chemical composition data in relation to two default dimensional axis (*NMDS*1 and *NMDS*2, see Figure 8), each color representing a specific necromass age. For this analysis all the wavelengths peaks displayed in Figure 4 were used. Considering that *NMDS*1 was the index that captured the most variation in the data, I observed that the spread of the data followed the chronological order in necromass ages, with a gradual difference in chemical composition following the growth patterns seen in Figure 3.

Furthermore, I observed clustering in between specific necromass ages groups. From the spatial analysis I could easily group necromass age 2 and 4, 8 and 15, and finally 29, 46, 67. This clustering could be linked to data in Figure 5, which displayed similar clusters based on the percentage of mass remaining during decomposition, at day 117. The NMDS analysis exposed that 86% of the variance of the data was explained through the necromass age treatment ($p_{\leq 0.05}$).

On the other hand, necromass age 8 in this NMDS analysis fell between the clustering of 8 and the "older" necromass ages group (29, 46, 67). I observed a point at coordinates $[0.45, -0.52]$ that had further spread and could be labelled as an outlier (as observed in Figure 8). I conducted a supplementary chemical composition analysis (FTIR) and found a similar result. Overall, the NMDS and PERMANOVA analysis showed a strong variation (86%, $p_{\leq 0.05}$) in fungal biomass biochemical composition depending on its physiological state at death, or necromass age.

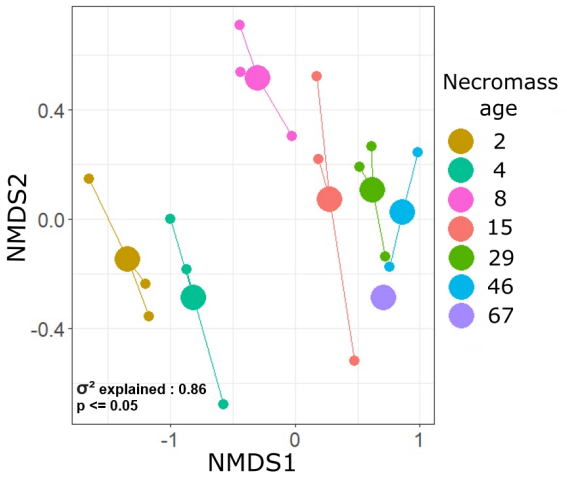

Figure 8: The initial necromass biochemical composition data obtained from the FTIR peak intensity (as shown in Table 4) was analyzed using Non-metric Multidimensional Scaling (NMDS) with necromass age treatment. 86% of the variance can be explained through necromass age treatment.

4.2.2 Functional Groups

Following multivariate analysis, I regrouped FTIR peaks based on the functional groups they had been assigned to (aliphatic, amide, polysaccharides, and aromatic, as shown in Table 4), and I analyzed these functional groups depending on *N. crassa* initial biomass physiological state or age (as shown in Figure 9).

First, aliphatic (a) functional group signal increased from "young" necromass age and peaked around intermediate necromass age 15, with a value of 5.5. Past this necromass age it decreased significantly, and then increased again until necromass age 67. Amide (b) functional group signal decreased gradually from “young” to “old” necromass age, starting around a value of 6.3, to then decreased significantly after necromass age 4, to finally reach a value of 4.2 around necromass age 67. The aromatic group (d) followed a similar trend, with functional group signal decreasing from "young" to "old" necromass age, from a signal value of 7.5 to 6.25. Furthermore, the polysaccharide group (c), encountered a gradual relative accumulation of polysaccharide-based compounds until necromass age 46, where it then decreased for necromass age 67. The way polysaccharides are behaving follows a pattern that’s quite like what I saw with ’A’ in the earlier section *3.1.3 Asymptotic Model Parameters*.

In summary, these results aligned with the multivariate analysis of *N. crassa* biomass composition demonstrating that the biochemical composition of mycelial biomass changed depending on its age or physiological states, with most changes explained by polysaccharide, amide, aliphatic and aromatic functional groups.

4.2.3 Carbon to Nitrogen Ratio in Relation to Necromass age.

To analyze further biochemical composition of *N. crassa* before incubation, I analyzed the fungal necromass C and N content and calculated C/N ratios (Figure 10). I observed a gradual increase of C/N ratio from necromass age 2 to necromass age 67, that respectively started at 6 and gradually reached 19. In other words, the C/N analysis showed that N concentration was higher in young necromass and decreased with age.

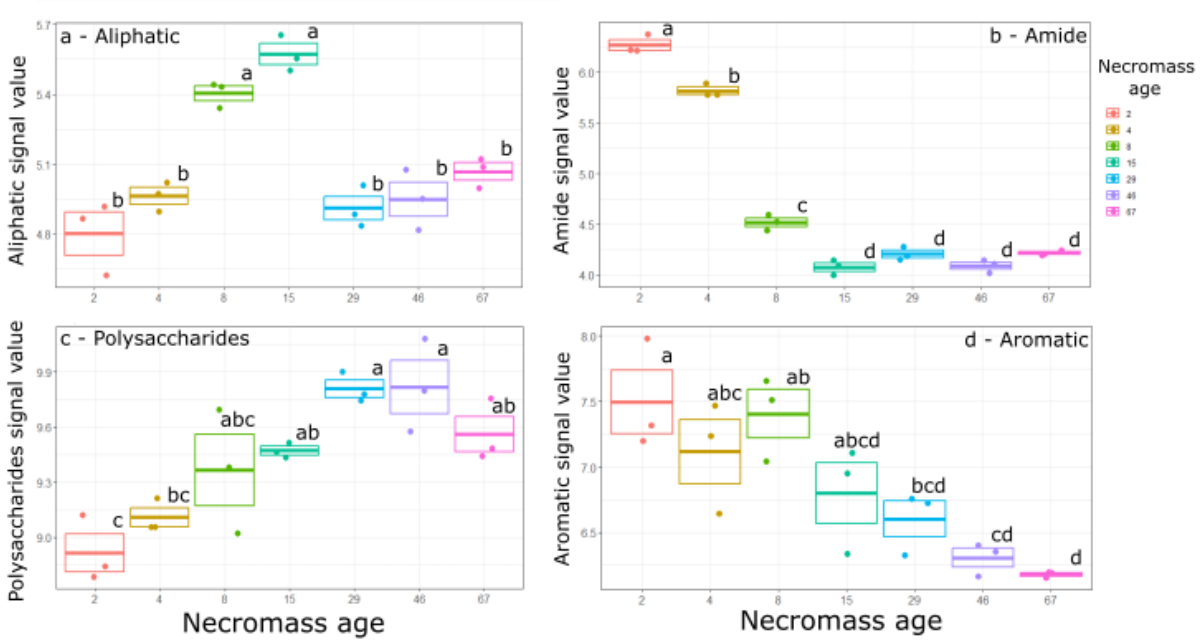

Figure 9: FTIR biochemical composition signal values over initial necromass ages, through different functional groups (a), (b), (c) and (d). Two wavelengths signals were summed for "Aliphatic", "Amide" and "Polysaccharide" groups, respectively (a), (b) and (c). Four wavelengths signals were summed for the "Aromatic" group, (d). For a better overview of the wavelengths selected for the functional groups, see Table 4. Letters a,b,c, and further combination represented results from the post hoc Tukey's test. Preliminary to the post hoc Tukey's test, a One-way ANOVA test was done on each functional group data, with aliphatic (a), amide (b), polysccharides (c) and aromatic (d). The p-values were respectively $p_{\leq 0.001}$ *(a),* $p_{\leq 0.001}$ *(b),* $p_{\leq 0.001}$ *(c) and* $p_{\leq 0.001}$ *(d).*

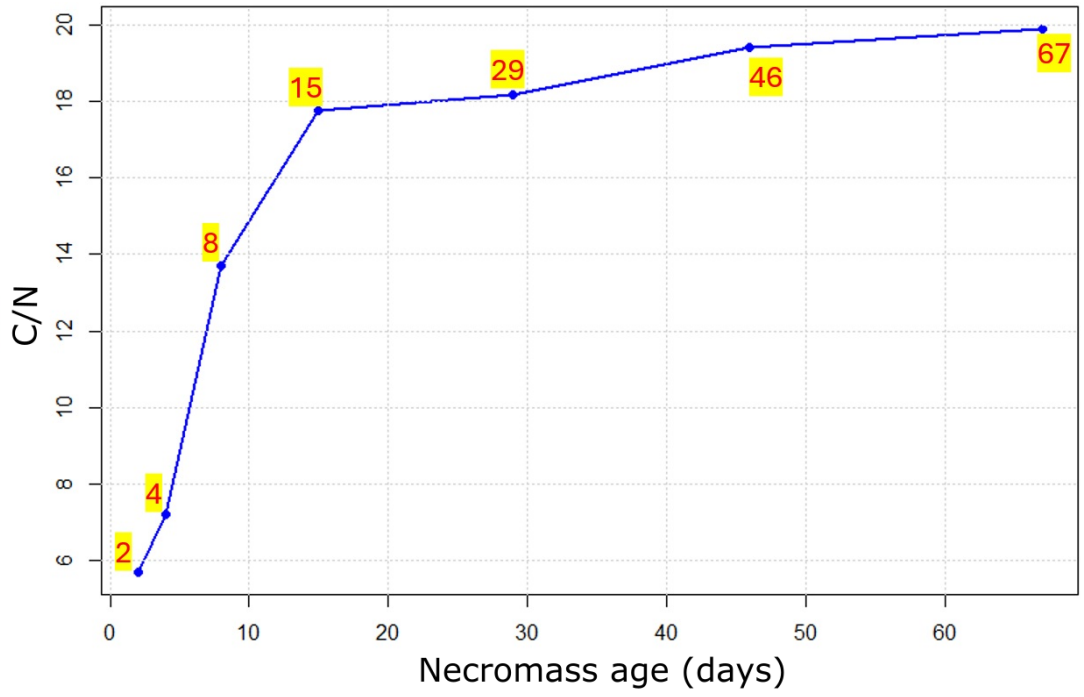

Figure 10: Carbon to Nitrogen ratio (C/N) depending on initial necromass age.

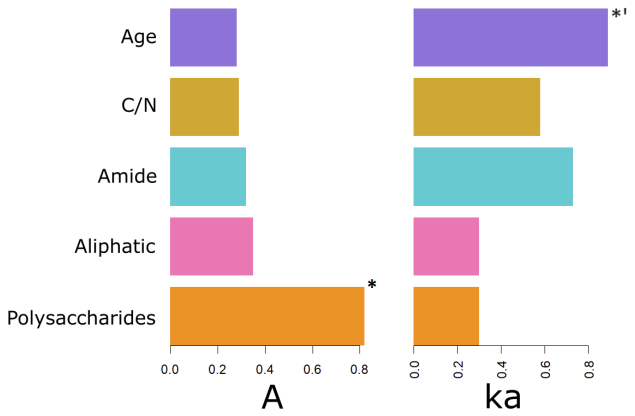

*Figure 11: Predictors weight plotted according to the independent variables (A, k_a) run throught the multi-model inference. * is a significant p-value inferior to 0.05. *' is a marginally significant p-value of 0.089.*

4.2.4 Predictor Analysis

Here, I attempted to predict fungal necromass decay parameters based on the fungal initial necromass biochemical composition. I used a multi-model inference approach with a list of potential predictors linked to the parameters of the necromass decomposition asymptotic model (A, k_a). After the model selection and averaging, I plotted each predictor's calculated weight based on their independent variable (as shown in Figure 11). Additionally, I plotted the preponderant predictor relationship with its corresponding asymptotic parameter (as shown in Figure 12).

On Figure 11 I observed for the asymptotes A calculated based on *N. crassa* necromass decomposition in soil, that polysaccharide was the main predictor with a weight value of 0.82, and a significant p-value (represented by "*", $p < 0.05$, F-statistics). Additionally, I observed that for the decay rates analysis (k_a), the main predictor was age with a weight value of 0.89, and a marginally significant p-value (represented by "*'", $p = 0.089$, F-statistics). Further, the analysis on the "A" independent variable makes a clear link between the A fraction decomposing at rate of 0, or recalcitrant, with the initial chemical concentration of polysaccharide in our necromass experiment. The relationship was positive, meaning that fungal necromass initially enriched in polysaccharides compounds based on FTIR spectroscopy presented high asymptotic remaining fraction values. In Figure 12 I plotted this relationship using a linear regression and mentioning the corresponding pearson coefficient value of 0.47. Overall, the multi-model inference approach allowed identification of the necromass biochemical predictors linked with decomposition parameters. Through this analysis, A was found better explained through the polysaccharide functional group and k_a (although marginally significant) was better explained through the physiological age at death.

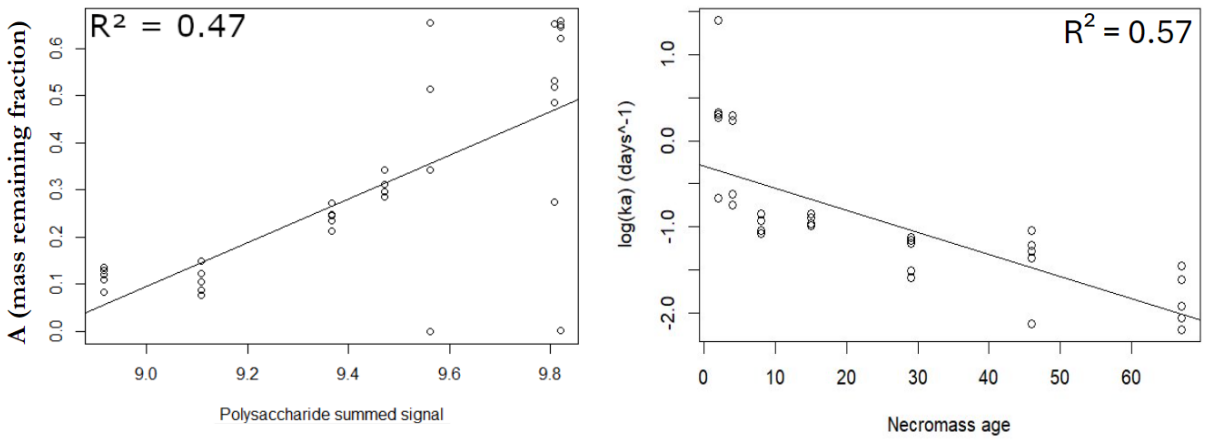

Figure 12: Graphs of best predictors (polysaccharides, necromass age) versus asymptotic model parameters (A, k_a).

4.3 Necromass Biochemical Changes During Decomposition

To analyse the relationships in our complex **decomposition** data by reducing its dimension, I chose to, similar to the analysis shown in Figure 8 analysis, use a Non-metric Multidimensional scaling (NMDS). Two NMDS analysis were conducted, one with a necromass age treatment and a second with decomposition time treatment, the analysis was summarized in Table 7, which includes the percentages of the variances explained and their corresponding p-value. After the multivariate analysis, I regrouped FTIR peaks based on the functional groups they have been assigned to (as shown in Table 4), and I plotted as shown in Figure 13 these functional groups signals depending on decomposition time (arranged per necromass ages), this was done to assess necromass biochemical changes in *N. crassa* during decomposition.

Previously, on the NMDS analysis of Table 8 (initial necromass), I had 86% of the variance explained through the necromass age arrangement criterion. However, in Table 7, I observed a smaller value of 50 % for necromass type treatment, which meant that when I considered the data spread through the lens of necromass age variable, I could only explain half of the variation during decomposition ($p_{\leq 0.05}$). However, when I only considered the decomposition time treatment, I noticed a variance value of 0.05, meaning that only 5% of the spread of the data could be explained trough the decomposition time criteria ($p_{\leq 0.05}$).

Turning our attention back to Figure 13, concerning aliphatic compounds (a), every necromass ages underwent some resistance in decomposition until t_{10}, resulting in an increase in signal value from t_0 to t_{10}. This did not mean that the necromass decomposing was gaining any aliphatic compounds through time. However, it meant that, relatively to the decomposition mass loss, the compound was not degraded in this initial stage and became more relatively abundant in comparison to other wavelengths signals sampled (b, c, d and other wavelengths in the range of 400-3800 nm). Further, the opposite trend was observed from t_{10} to t_{46} where the signal was decreasing for all the necromass ages, meaning that most of the sampled compounds linked to those wavelengths were getting degraded and appeared relatively less present in the chemical composition. Aside from necromass age 2 and 4 which ended up increasing their signal value from t_0 to t_{117}, the rest of the necromass ages remained stable in signal, although they went through fluctuations during the decomposition phase. Regarding amide compounds (b), every necromass age underwent a significant degradation step from t_0 to t_{10}, and a resilient step mostly from t_{10} to t_{20}, but overall the signal values intensity remained quite close to the initial t_0 values.

Here the necromass of age 15 and 67 underwent relative increase in their signal value of amide compound from t_0. As for polysaccharides (c), necromass ages 8, 29, 46 and 67 were relatively stable in their relative abundance during decomposition. However, necromass ages 2 and 4, (and especially 2) underwent a significant relative decrease in their signal value of polysaccharide compounds from t_0. Finally, aromatic (d),there was a quite a relative stable signal intensity in aromatic compounds for "older" necromass, respectively necromass age 29,46 and 67. However, the more "younger" necromass, from age 2 until 15, had a significant decrease of relative signal from t_0 to t_{10}, meaning that in those necromass ages, some aromatic compounds channeled by the selected wavelengths are highly deteriorated from decomposition. The signals were then more stable until t_{76}. Past that time stamp only necromass age 2 was further decreasing in relative concentration.

Overall, the NMDS analysis on necromass biochemical changes during decomposition explained 50% of the variation through necromass age treatment, but only 5% through the decomposition time. Additionally, our FTIR results showed that "older" necromass had a rather stable decomposition pattern through (a),(b),(c) and (d). In comparison to that "younger" necromass ages, especially the necromass ages 2 and 4, got sensible relative increase in signal in compounds of aliphatic (a), however they decreased significantly in polysaccharide (c) and aromatic (d).

Table 7: Non-metric Multidimensional Scaling (NMDS), using the following arrangement criteria, necromass age (a), decomposition time (b). The data used is from the decomposition chemical composition change gathered from the FTIR analysis.

NMDS decomposition results	Necromass type treatment	Decomposition time treatment
Variance	0.5	0.05
p-value significance	$p \leq 0.05$	$p \leq 0.05$

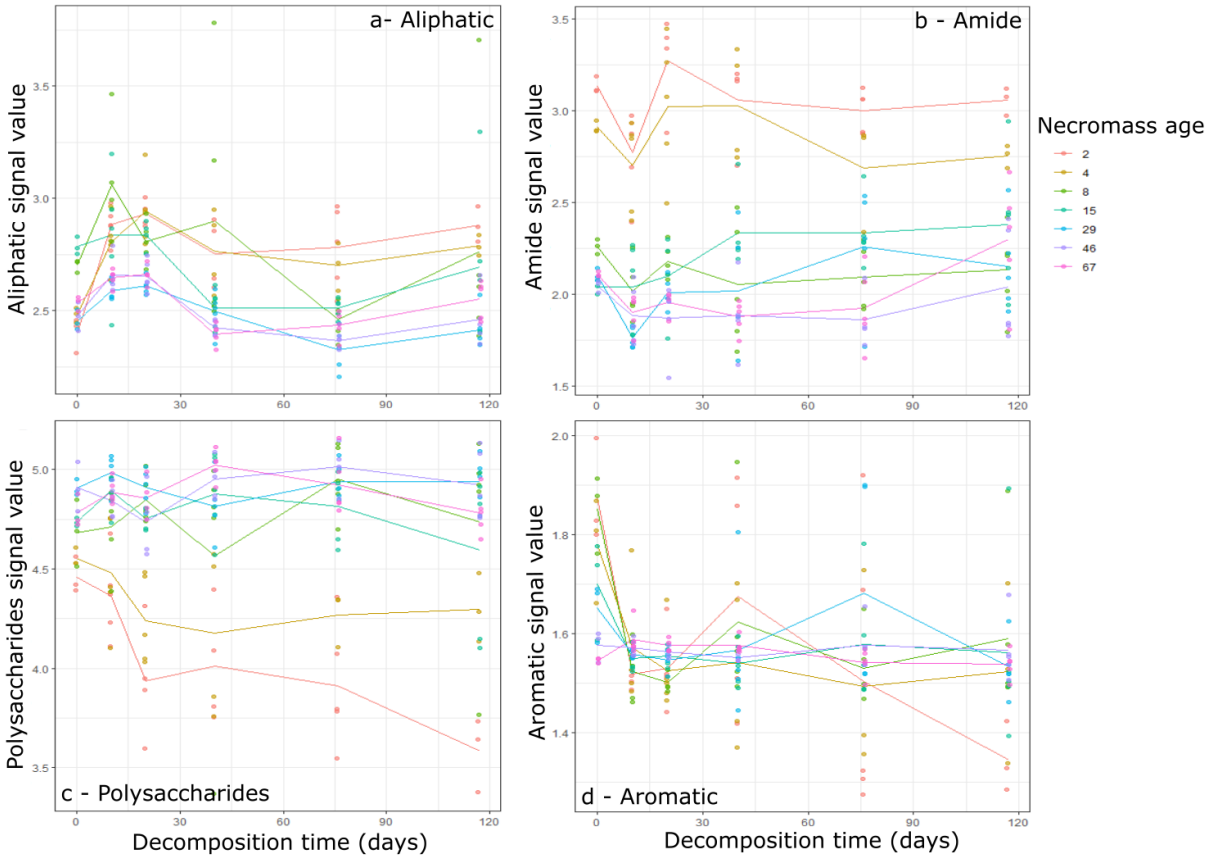

Figure 13: FTIR biochemical signal values depending on decomposition time (arranged per necromass ages). Different functional groups (a),(b),(c) and (d) were addressed through this FTIR analysis (as shown in Table 4). Signal values were averaged (lines), and independent wavelength signal were added (dots).

5 Discussion

In our experiment, *N. crassa* necromass decomposing in soils underwent an initial phase of rapid mass loss followed by a plateau phase, a trend consistently observed in other studies on fungal necromass (See et al., 2021; Brabcová et al., 2016; Maillard et al., 2021; Fernandez et al., 2020). In terms of decay models, I found that fungal necromass was best represented by an asymptotic model, independent of the fungal necromass age at death. This model superseded the single exponential representation and provided an overview of a fast pool with more labile compounds, expressed through the decay rate k_a, followed by a slow pool with a decay rate close to zero, expressed through an asymptote A. Our results aligned with recent literature describing fungal necromass decay using an asymptotic model (See et al., 2021; Maillard et al., 2021). However, they contradicted previous studies that assumed a constant decay rate for fungal necromass decomposition and used a single exponential model to represent these processes in soil C and subsequent modeling (Fernandez and Koide, 2014; Sulman et al., 2014, 2017).

In terms of soil biochemical processes, this indicates two distinct phases during fungal necromass decomposition: The first phase, dominated by high decay rates (k_a), likely involves the rapid transfer of necromass-C into microbial decomposer biomass and subsequent respiration and emission as CO_2. The second, asymptotic phase (A), involves most remaining necromass-C becoming stable in soils and contributing to SOC stocks.

In agreement with our hypotheses, I identified the fungal age or physiological state at time of death as an important factor in fungal necromass decay dynamics. While fungal necromass mass remaining at the end of decomposition ranges from 8 to 30% between species with contrasting biochemical compositions, I identified variation ranging from 8 to 50% within a single fungal species (*Neurospora crassa*) killed at different physiological stages. Specifically, both fungal necromass decay rates and persistent fractions, or asymptotes, varied greatly depending on mycelial age at death. However, model decay parameters (A, k_a) did not follow a linear relationship with fungal age at death. For example, while decay rate values gradually decreased with fungal biomass age at death, the persistent fraction (A) peaked at 46 days of growth for the model fungal species studied, before declining after 67 days of growth. This indicates that while fungal age at death is an important factor in fungal necromass decay dynamics, a complex relationship exists between necromass decomposition and the fungal physiological state at death.

Collectively, this suggests that if most fungal mycelium in soil dies at a young age, most of the necromass-C will be transformed either into microbial biomass or emitted as CO_2 post-mineralization. Conversely, if fungal biomass dies at an intermediate age (around age 15, 29), most of the necromass-C might persist in soil as POM. This highlights the physiological state at death of soil fungal species as a likely key driver in the formation of particulate organic C of fungal origin. There is still a lot I don't understand about how fungi die in the soil. To make our findings more useful in understanding soil carbon biogeochemistry, I need to focus on this topic in future research.

Interestingly, the strong effect of fungal mycelium age at death on decay dynamics I observed has not been previously described in the literature. However, comparing the necromass decomposition of various fungal species, See et al. (2021) found that the biochemical composition of the fungal necromass was an important factor in decomposition rates and mass remaining fractions. Thus, I speculate that the necromass age effect observed for *N. crassa* is due to mycelium aging processes that induce biochemical differences in biomass composition. Our findings indicate that the biochemical composition of necromass varies with necromass age.

Specifically, I observed that younger necromass residues have a higher concentration of amides, likely linked with proteins. Additional data brought by C/N ratio analysis also supports this finding. In contrast, the concentration of polysaccharides in the initial necromass gradually increases with age, following a nearly linear relationship, until peaking at age 46.

Fungal necromass mass remaining at the end of decomposition in our experiment was strongly predicted by the initial content of polysaccharide compounds within *N. crassa* biomass. As such, the resistance of intermediate-aged *N. crassa* necromass (29 to 46 days of growth) in soil could be explained by a relatively higher fraction of structural compounds, such as polysaccharides composing the fungal cell wall, likely chitin and glucan, when compared with younger residues. The effect of polysaccharide content appears significantly more precise in describing the remaining fraction after decomposition (A) compared to the physiological age at death of *N. crassa*. This further supports our speculation of necromass biochemical differences induced by mycelium aging processes. Previous literature describes a portion of polysaccharide compounds as linked with fungal structural cell wall components, specifically glycosidic groups or glucan complexes (Chandran et al., 2016; Heidrich et al., 2021). This means that glycosidic and glucan complexes, usually present in cell walls, could be components in the polysaccharide group that are highly resistant to microbial decomposition in soils. It is nevertheless rather surprising that old necromass was found to not present the highest remaining necromass mass at the end of decomposition. I speculate that *N. crassa* might have started recycling its cell wall post-46 days of growth, as highlighted by biomass losses between 46 and 67 days of in vitro growth, leading to a decrease in polysaccharides quantified by FTIR.

While fungal necromass mass remaining at the end of decomposition was well predicted by polysaccharide content in fungal necromass before soil incubation, the initial decay rates were only marginally explained by necromass age at death, with younger necromass types presenting higher decay rates. This may suggest that FTIR applied to fungal necromass might not be the best method to assess the labile fraction of fungal residues. Importantly, the C/N ratio, often used as a predictor of decay dynamics in leaf and wood decomposition studies, did not have any significant predictive power in our study for either fungal necromass decay rates or mass remaining at the end of decomposition. This indicates that in-depth biochemical characterization of fungal necromass pre-incubation is needed to understand the drivers of fungal necromass decay. Altogether, our results point to fungal mycelial biochemical changes induced by aging processes or responses to C and nutrient availability in the medium, indicating that the fungal physiological state is a key driver in fungal necromass decomposition in soils. This finding supersedes all other identified drivers, such as inter-species biochemical differences (See et al., 2021), soil or plant parameters (Maillard et al., 2023b), and vegetation types (Beidler et al., 2020).

I assessed the chemical changes in fungal necromass during decomposition using FTIR. Surprisingly, I found only minor biochemical changes in *N. crassa* necromass during decomposition, with decomposition time accounting for just a few percent (5%) of the biochemical variation, compared to 50% explained by the biomass age at death. Limited biochemical changes during decomposition have also been observed by Maillard et al. (2023b) using FTIR, where both lowly and highly melanized fungal residue FTIR profiles showed marginal changes during decomposition. Similarly, Ryan et al. (2020) found relatively small biochemical changes in fungal necromass from three different fungal species using Py-GCMS, with an increase in the aliphatic (or lipid) fraction relative to the polysaccharide or carbohydrate fraction. These findings support our results and suggest a consistent rate of decomposition for different compounds in

fungal necromass. Therefore, by comparing the magnitude of biochemical changes at the time of death with those during decomposition, I propose that these changes are more closely linked to the physiological state of the fungus at death rather than to microbial decomposers specifically targeting one compound group over another during fungal necromass decay.

6 Limitation and future directions

See et al. (2021), Brabcová et al. (2016), and Fernandez and Koide (2014), along with our own study, all provide valuable insight with comparable meshbag experimental design. These studies share a limitation of having a short experiment duration. To determine the actual duration of the slow pool fraction (A), multiple-year studies are needed to further address this question. Additionally, studies using other fungi species of interest and different experiment designs are challenging to compare. Our study and See et al. (2021) used different experimental designs, with ours conducted in the field and theirs in a controlled environment, resulting in non-identical decomposition conditions. Finally, it would be beneficial to explore more intricate modeling techniques that are currently being utilized in plant litter research, as mentioned in the study by Gill et al. (2021). By doing so, the implementation of double exponential and weibull models could potentially provide a more in-depth and advanced approach beyond traditional asymptotic modeling representations.

7 Conclusion

This study investigated how the physiological state at death affects the decomposition of *Neurospora crassa* necromass. Our results demonstrated that fungal necromass decomposition follows an asymptotic model, with initial rapid mass loss followed by a plateau phase. I found that *N. crassa* physiological age at death significantly influences decomposition dynamics, with intermediate-aged necromass exhibiting greater resistance likely due to higher polysaccharide content. These findings support that fungal physiological state at death is likely a key driver in soil C cycling with some fungal necromass ages more likely to contribute to the formation of soil organic carbon than others. Our results indicate that fungal necromass age or physiological state at death is a critical factor in decay dynamics, surpassing inter-species biochemical differences and environmental factors. I observed that younger necromass decomposes faster, whereas intermediate-aged necromass persists longer in the soil. However, additional research is needed to explore long-term decomposition and incorporate our findings into soil carbon models. This study underscores the importance of considering fungal physiological state at death when investigating fungal necromass decomposition and its role in SOC formation.

References

Abdi, H. and Williams, L. J. (2010). Newman-keuls test and tukey test. *Encyclopedia of research design*, 2:897–902.

Angst, G., Angst, Š., Frouz, J., Jabinski, S., Jílková, V., Kukla, J., Li, M., Meador, T. B., and Angel, R. (2024). Stabilized microbial necromass in soil is more strongly coupled with microbial diversity than the bioavailability of plant inputs. *Soil Biology and Biochemistry*, 190:109323.

Angst, G., Mueller, K. E., Nierop, K. G., and Simpson, M. J. (2021). Plant-or microbial-derived? a review on the molecular composition of stabilized soil organic matter. *Soil Biology and Biochemistry*, 156:108189.

Beidler, K. V., Phillips, R. P., Andrews, E., Maillard, F., Mushinski, R. M., and Kennedy, P. G. (2020). Substrate quality drives fungal necromass decay and decomposer community structure under contrasting vegetation types. *Journal of Ecology*, 108(5):1845–1859.

Blaschke, M., Siemonsmeier, A., Harjes, J., Okach, D. O., and Rambold, G. (2023). Comparison of survey methods for fungi using metabarcoding and fruit body inventories in an altitudinal gradient. *Archives of Microbiology*, 205(7):269.

Brabcová, V., Nováková, M., Davidová, A., and Baldrian, P. (2016). Dead fungal mycelium in forest soil represents a decomposition hotspot and a habitat for a specific microbial community. *New Phytologist*, 210(4):1369–1381.

Brethauer, S., Shahab, R. L., and Studer, M. H. (2020). Impacts of biofilms on the conversion of cellulose. *Applied microbiology and biotechnology*, 104:5201–5212.

Bruker Corporation (2023). OPUS Software. `https://www.bruker.com/en/products-and-solutions/infrared-and-raman/opus-spectroscopy-software.html`. Accessed: 2023-01-28.

Buckeridge, K. M., Mason, K. E., Ostle, N., McNamara, N. P., Grant, H. K., and Whitaker, J. (2022). Microbial necromass carbon and nitrogen persistence are decoupled in agricultural grassland soils. *Communications Earth & Environment*, 3(1):114.

Burnham, K. P. and Anderson, D. R. (2002). *Model selection and multimodel inference: a practical information-theoretic approach*. Springer.

Camenzind, T., Mason-Jones, K., Mansour, I., Rillig, M. C., and Lehmann, J. (2023). Formation of necromass-derived soil organic carbon determined by microbial death pathways. *Nature geoscience*, 16(2):115–122.

Certano, A. K., Fernandez, C. W., Heckman, K. A., and Kennedy, P. G. (2018). The after-life effects of fungal morphology: Contrasting decomposition rates between diffuse and rhizomorphic necromass. *Soil Biology and Biochemistry*, 126:76–81.

Chai, T. and Draxler, R. R. (2014). Root mean square error (rmse) or mean absolute error (mae)?–arguments against avoiding rmse in the literature. *Geoscientific model development*, 7(3):1247–1250.

Chandran, M., Mangaleshwari, R., Udhayavani, K., and Murugan, K. (2016). Studies on ftir analysis of fraction i and ii of annonasquamosa methanol leaf extract. *World journal of pharmacy and pharmaceutical sciences*, 5(8):1247–1256.

Chen, X., Ni, X., Zheng, G., Hu, M., and Chen, H. Y. (2024). Changes in plant lignin components and microbial necromass matter with subtropical forest restoration. *Geoderma*, 445:116875.

Cocozza, C., D'Orazio, V., Miano, T., and Shotyk, W. (2003). Characterization of solid and aqueous phases of a peat bog profile using molecular fluorescence spectroscopy, esr and ft-ir, and comparison with physical properties. *Organic Geochemistry*, 34(1):49–60.

Cotrufo, M. F. and Lavallee, J. M. (2022). Soil organic matter formation, persistence, and functioning: A synthesis of current understanding to inform its conservation and regeneration. *Advances in agronomy*, 172:1–66.

Fernandez, C. W., Heckman, K., Kolka, R., and Kennedy, P. G. (2019). Melanin mitigates the accelerated decay of mycorrhizal necromass with peatland warming. *Ecology Letters*, 22(3):498–505.

Fernandez, C. W. and Kennedy, P. G. (2018). Melanization of mycorrhizal fungal necromass structures microbial decomposer communities. *Journal of Ecology*, 106(2):468–479.

Fernandez, C. W. and Koide, R. T. (2014). Initial melanin and nitrogen concentrations control the decomposition of ectomycorrhizal fungal litter. *Soil Biology and Biochemistry*, 77:150–157.

Fernandez, C. W., See, C. R., and Kennedy, P. G. (2020). Decelerated carbon cycling by ectomycorrhizal fungi is controlled by substrate quality and community composition. *New Phytologist*, 226(2):569–582.

Fontana, J. D. and Krisman, C. R. (1978). Glycogen synthesis in the fungus neurospora crassa. *Biochimica et Biophysica Acta (BBA)-General Subjects*, 540(2):183–189.

Geogebra (2024). GeoGebra. Accessed: 2024-01-29.

Gill, A. L., Schilling, J., and Hobbie, S. E. (2021). Experimental nitrogen fertilisation globally accelerates, then slows decomposition of leaf litter. *Ecology Letters*, 24(4):802–811.

Heidrich, D., Koehler, A., Ramírez-Castrillón, M., Pagani, D. M., Ferrão, M. F., Scroferneker, M. L., and Corbellini, V. A. (2021). Rapid classification of chromoblastomycosis agents genera by infrared spectroscopy and chemometrics supervised by sequencing of rdna regions. *Spectrochimica Acta Part A: Molecular and Biomolecular Spectroscopy*, 254:119647.

Hobbie, S. E. (2008). Nitrogen effects on decomposition: A five-year experiment in eight temperate sites. *Ecology*, 89(9):2633–2644.

Hodson, T. O. (2022). Root mean square error (rmse) or mean absolute error (mae): When to use them or not. *Geoscientific Model Development Discussions*, 2022:1–10.

Jandl, R., Lindner, M., Vesterdal, L., Bauwens, B., Baritz, R., Hagedorn, F., Johnson, D. W., Minkkinen, K., and Byrne, K. A. (2007). How strongly can forest management influence soil carbon sequestration? *Geoderma*, 137(3-4):253–268.

Kim, T. K. (2017). Understanding one-way anova using conceptual figures. *Korean journal of anesthesiology*, 70(1):22.

Kuo, H.-C., Hui, S., Choi, J., Asiegbu, F. O., Valkonen, J. P., and Lee, Y.-H. (2014). Secret lifestyles of neurospora crassa. *Scientific Reports*, 4(1):5135.

Lal, R. (2004). Soil carbon sequestration to mitigate climate change. *Geoderma*, 123(1-2):1–22.

Lal, R. (2016). Soil health and carbon management. *Food and Energy Security*, 5(4):212–222.

Liang, C., Amelung, W., Lehmann, J., and Kästner, M. (2019). Quantitative assessment of microbial necromass contribution to soil organic matter. *Global change biology*, 25(11):3578–3590.

Maillard, F., Beatty, B., Park, M., Adamczyk, S., Adamczyk, B., See, C. R., Cavender-Bares, J., Hobbie, S. E., and Kennedy, P. G. (2023a). Microbial community attributes supersede plant and soil parameters in predicting fungal necromass decomposition rates in a 12-tree species common garden experiment. *Soil Biology and Biochemistry*, 184:109124.

Maillard, F., Fernandez, C. W., Mundra, S., Heckman, K. A., Kolka, R. K., Kauserud, H., and Kennedy, P. G. (2022). Warming drives a 'hummockification'of microbial communities associated with decomposing mycorrhizal fungal necromass in peatlands. *New Phytologist*, 234(6):2032–2043.

Maillard, F., Kennedy, P. G., Adamczyk, B., Heinonsalo, J., and Buée, M. (2021). Root presence modifies the long-term decomposition dynamics of fungal necromass and the associated microbial communities in a boreal forest. *Molecular ecology*, 30(8):1921–1935.

Maillard, F., Pflender, S., Heckman, K. A., Chalot, M., and Kennedy, P. G. (2023b). Fungal necromass presents a high potential for mercury immobilization in soil. *Chemosphere*, 311:136994.

Mancinelli, R., van Bodegom, P., Lankhorst, J., and Soudsilovskaia, N. (2023). Understanding the impact of main cell wall polysaccharides on the decomposition of ectomycorrhizal fungal necromass. *European Journal of Soil Science*, 74(2):e13351.

Microsoft Corporation (2023). Microsoft Excel. `https://www.microsoft.com/en-us/microsoft-365/excel`. Accessed: 2023-03-22.

Niemeyer, J., Chen, Y., and Bollag, J.-M. (1992). Characterization of humic acids, composts, and peat by diffuse reflectance fourier-transform infrared spectroscopy. *Soil Science Society of America Journal*, 56(1):135–140.

Olson, J. S. (1963). Energy storage and the balance of producers and decomposers in ecological systems. *Ecology*, 44(2):322–331.

Ostrowska, A. and Porębska, G. (2015). Assessment of the c/n ratio as an indicator of the decomposability of organic matter in forest soils. *Ecological Indicators*, 49:104–109.

Pérez-Pazos, E., Beidler, K. V., Narayanan, A., Beatty, B. H., Maillard, F., Bancos, A., Heckman, K. A., and Kennedy, P. G. (2024). Fungi rather than bacteria drive early mass loss from fungal necromass regardless of particle size. *Environmental microbiology reports*, 16(3):e13280.

RStudio Team (2024). *RStudio: Integrated Development Environment for R*. RStudio, PBC., Boston, MA.

Ryan, M. E., Schreiner, K. M., Swenson, J. T., Gagne, J., and Kennedy, P. G. (2020). Rapid changes in the chemical composition of degrading ectomycorrhizal fungal necromass. *Fungal ecology*, 45:100922.

Schmidt, M. W., Torn, M. S., Abiven, S., Dittmar, T., Guggenberger, G., Janssens, I. A., Kleber, M., Kögel-Knabner, I., Lehmann, J., Manning, D. A., et al. (2011). Persistence of soil organic matter as an ecosystem property. *Nature*, 478(7367):49–56.

See, C. R., Fernandez, C. W., Conley, A. M., DeLancey, L. C., Heckman, K. A., Kennedy, P. G., and Hobbie, S. E. (2021). Distinct carbon fractions drive a generalisable two-pool model of fungal necromass decomposition. *Functional Ecology*, 35(3):796–806.

Sulman, B. N., Brzostek, E. R., Medici, C., Shevliakova, E., Menge, D. N., and Phillips, R. P. (2017). Feedbacks between plant n demand and rhizosphere priming depend on type of mycorrhizal association. *Ecology letters*, 20(8):1043–1053.

Sulman, B. N., Phillips, R. P., Oishi, A. C., Shevliakova, E., and Pacala, S. W. (2014). Microbe-driven turnover offsets mineral-mediated storage of soil carbon under elevated co2. *Nature Climate Change*, 4(12):1099–1102.

Sussman, A. S. (2013). Longevity and survivability of fungi. *The fungi*, 3:447–486.

Thevelein, J. (1984). Regulation of trehalose mobilization in fungi. *Microbiological reviews*, 48(1):42–59.

Turner, B. C., Perkins, D. D., and Fairfield, A. (2001). Neurospora from natural populations: a global study. *Fungal Genetics and Biology*, 32(2):67–92.

Vega, K., Kalkum, M., et al. (2012). Chitin, chitinase responses, and invasive fungal infections. *International journal of microbiology*, 2012.